HHS Public Access

Author manuscript

Brain Behav Immun. Author manuscript; available in PMC 2023 March 01.

Published in final edited form as:

Brain Behav Immun. 2022 March ; 101: 304–317. doi:10.1016/j.bbi.2022.01.004.

Subfornical organ interleukin 1 receptor: A novel regulator of spontaneous and conditioned fear associated behaviors in mice

Katherine M.J. McMurray[a,d], **Andrew Winter**[a,b], **Rebecca Ahlbrand**[a], **Allison Wilson**[c], **Sachi Shukla**[c], **Renu Sah**[a,b,d,*]

[a] Department of Pharmacology and Systems Physiology, University of Cincinnati, USA

[b] Neuroscience Graduate Program, University of Cincinnati, USA

[c] Neuroscience Undergraduate Program, University of Cincinnati, USA

[d] Veterans Affairs Medical Center, Cincinnati, OH, USA

Abstract

Impaired threat responding and fear regulation is a hallmark of psychiatric conditions such as post-traumatic stress disorder (PTSD) and Panic Disorder (PD). Most studies have focused on external psychogenic threats to study fear, however, accumulating evidence suggests a primary role of homeostatic perturbations and interoception in regulating emotional behaviors. Heightened reactivity to interoceptive threat carbon dioxide (CO_2) inhalation associates with increased risk for developing PD and PTSD, however, contributory mechanisms and molecular targets are not well understood. Previous studies from our group suggested a potential role of interleukin 1 receptor (IL-1R1) signaling within BBB-devoid sensory circumventricular organ, the subfornical organ (SFO) in CO_2-evoked fear. However, the necessity of SFO-IL-1R1 in regulating CO_2-associated spontaneous fear as well as, long-term fear potentiation relevant to PD/PTSD has not been investigated. The current study tested male mice with SFO-targeted microinfusion of the IL-1R1 antagonist (IL-1RA) or vehicle in a recently developed CO_2-startle-fear conditioning-extinction paradigm. Consistent with our hypothesis, SFO IL-1RA treatment elicited significant attenuation of freezing and increased rearing during CO_2 inhalation suggesting SFO-IL1R1 regulation of spontaneous fear to CO_2. Intriguingly, SFO IL-1RA treatment normalized CO_2-associated potentiation of conditioned fear and impaired extinction a week later suggesting modulation of long-term fear by SFO-IL-1R1 signaling. Post behavior FosB mapping revealed recruitment of prefrontal cortex-amygdala-periaqueductal gray (PAG) areas in SFO-IL-1RA mediated effects. Additionally, we localized cellular IL-1R1 expression within the SFO to blood vessel endothelial

* Corresponding author at: Dept. of Pharmacology & Systems Physiology, University of Cincinnati, UC North Reading Campus, 2170 East Galbraith Road, Cincinnati, OH 45237. sahr@uc.edu (R. Sah).

Author Contributions

KMJM conceived of project, collected and analyzed all behavioral and tissue data and wrote the paper. AW (Winter) conducted IL-1R expression in transgenic mice, RA assisted with tissue collection and processing for qPCR data, AW (Wilson) assisted with behavioral scoring, SS assisted with FosB quantification. RS conceived of project, acquired funding, advised project design, data interpretation, and wrote the paper.

Declaration of Competing Interest

The authors declare that they have no known competing financial interests or personal relationships that could have appeared to influence the work reported in this paper.

Appendix A. Supplementary data

Supplementary data to this article can be found online at https://doi.org/10.1016/j.bbi.2022.01.004.

cells and observed CO_2-induced alterations in IL-1β/IL-1R1 expression in peripheral mononuclear cells and SFO. Lastly, CO_2-evoked microglial activation was attenuated in SFO-IL-1RA treated mice. These observations suggest a peripheral monocyte-endothelial-microglia interplay in SFO-IL-1R1 modulation of CO_2-associated spontaneous fear and delayed fear memory. Collectively, our data highlight a novel, "bottom-up" neuroimmune mechanism that integrates interoceptive and exteroceptive threat processing of relevance to fear-related pathologies.

Keywords

IL-1R1; Subfornical organ; Fear; Threat; CO_2; Panic; PTSD

1. Introduction

Fear is a universal response to threat that engages defensive behaviors to ensure safety and survival. Maladaptive threat responding is associated with fear-related disorders such as posttraumatic stress disorder (PTSD) and panic disorder. Most of our current mechanistic understanding of fear is based on defensive responding to aversive external threats. However, mounting evidence supports a primary role of homeostasis and interoception: "an individual's sensing and monitoring of the physiological condition of the body itself" in regulation of emotional behaviors and memory (Pfeifer et al., 2017; Khalsa et al., 2018; Damasio and Carvalho, 2013). Consistently, individuals with panic disorder and PTSD show increased emotional reactivity to homeostatic triggers such as sodium lactate and carbon dioxide (CO_2) inhalation (Wemmie, 2011; Muhtz et al., 2012; Vollmer et al., 2015; Kellner et al., 2018). Exposure to CO_2 produces intense fear-associated behavioral and physiological responses in humans and rodents (Leibold et al., 2016; Ziemann et al., 2009; McMurray et al., 2020; Rassovsky and Kushner, 2003; Vollmer et al., 2016; McMurray et al., 2019), and can modulate long-term reactivity to subsequent psychogenic stressors (McMurray et al., 2020; Telch et al., 2012). Interestingly, heightened emotional responses to CO_2 may exist prior to PTSD and panic diagnosis, highlighting CO_2 sensitivity as a risk factor for these disorders (Telch et al., 2012; Coryell et al., 2006). Mounting evidence within clinical and preclinical studies points to neuroimmune signaling in pathologies associated with CO_2 sensitivity like PTSD and panic disorder (Vollmer et al., 2016; Michopoulos et al., 2017; Sumner et al., 2020; Won and Kim, 2020; Deslauriers et al., 2018; Jones et al., 2015; Furtado and Katzman, 2015). Limited studies have investigated the direct role of neuroimmune signaling in mediating CO_2 responsivity and lasting CO_2-dependent effects, nor the central nodes through which this signaling acts (Vollmer et al., 2016; van Duinen et al., 2008; Marques et al., 2021).

Our recent work reported a role for the subfornical organ (SFO) in facilitating CO_2-evoked fear (Vollmer et al., 2016). The SFO is a sensory circumventricular organ (CVO) located near the lateral ventricle and lacks a typical blood brain barrier (BBB), enabling access to systemic and CNS compartments for sensing the internal milieu (Johnson and Gross, 1993). The SFO has a well-recognized role as a chemosensory locus for detecting perturbations in systemic homeostasis for regulation of thirst and salt appetite (McKinley et al., 2019; Matsuda et al., 2017), autonomic state (Smith and Ferguson, 2010) and immune responses

(Sisó et al., 2010). Additionally, our work suggested that neuroimmune signaling within the SFO is engaged during exposure to homeostatic trigger CO_2 inhalation. We found CO_2 inhalation increased activation of SFO microglia and CO_2-evoked neuronal firing in patch-clamped SFO neurons was dependent on IL-1R1 signaling (Vollmer et al., 2016). Central infusion of interleukin 1 (IL-1) receptor antagonist (IL-1RA) attenuated CO_2-evoked freezing in mice (Vollmer et al., 2016). Though suggestive of SFO-mediated effects, the necessity of SFO IL-1R1 in mediating acute, spontaneous responses to CO_2 inhalation was not established. Additionally, it is unclear whether CO_2 effects on SFO or IL-1R1 could also drive the potentiation of fear responding to subsequent stressors that may underlie risk for developing pathology (McMurray et al., 2020). Currently, most studies on IL-1R mediated regulation of fear has focused on traditional fear circuits, primarily via the hippocampus (Jones et al., 2015; Goshen et al., n.d; Jones et al., 2018; Rachal Pugh et al., 2001). Given the SFO's strategic neuronal projections to forebrain areas regulating defensive behaviors (Swanson and Lind, 1986; Miselis, 1981), engagement of IL-1R signaling within this interoceptive, chemosensory site may represent a unique integrative site where threatful homeostatic signals can be sensed and translated into fear responsive behaviors.

With all these considerations in mind, the current study was undertaken to a) determine whether IL-1R1 signaling within the SFO is necessary for regulating spontaneous and conditioned behaviors to CO_2, and b) investigate whether SFO-IL-1R1 is recruited in delayed effects of CO_2 inhalation on defensive responding to subsequent exteroceptive triggers. To investigate the integration of threat responding to interoceptive and exteroceptive cues, we used a recently developed paradigm where mice are exposed to CO_2 or air inhalation and tested one week later for acoustic startle and foot shock contextual fear conditioning, extinction and reinstatement (McMurray et al., 2020). Prior CO_2 exposure associates with potentiated conditioned fear and delayed extinction via disruptions in amygdala-prefrontal activation (McMurray et al., 2020). Based on previous observations, (McMurray et al., 2020; Vollmer et al., 2016), our hypothesis was that IL-1R1 within the SFO represents a facilitator of defensive responding to interoceptive threat CO_2, and also mediates the long-term effects of prior CO_2 inhalation on later contextual fear memory. We utilized site-specific microinfusion of IL-1R1 antagonist, IL-1RA, in the SFO to test acute spontaneous defensive responding to CO_2 inhalation and delayed potentiation of contextual fear memory. Given our previous data on the recruitment of SFO microglia in CO_2-evoked fear (Vollmer et al., 2016), we assessed microglial alterations in SFO-IL-1RA infused mice. Furthermore, to elucidate downstream regional recruitment in SFO-IL-1RA regulation of fear, we conducted post behavior alterations in delta FosB, a surrogate marker for sustained neuronal activation in primary forebrain-midbrain areas that regulate fear-associated defensive behaviors. Additionally, we localized cellular IL-1R1 expression within the SFO to endothelial cells and investigated CO_2-induced regulation of IL-1β/IL1-R1 in SFO and peripheral monocytes implicated in stress-associated behavioral regulation (McKim et al., 2018). Our data suggest that IL-1R1 signaling within the SFO regulates acute threat responding to interoceptive trigger, CO_2, as well as effects of prior CO_2 inhalation on later contextual fear memory via cortico-amygdala-periaqueductal gray integration.

2. Methods and materials

2.1. Animals

Studies were performed using 8 week old, male BALB/c mice (Envigo, Indianapolis, IN), consistent with age, sex and strain used in previous studies from our lab on the effects of CO_2 inhalation on fear behavior and the SFO (McMurray et al., 2020; Vollmer et al., 2016; McMurray et al., 2019; Winter et al., 2019). To characterize cell-type-specific IL-1R1 expression in the SFO, transgenic reporter mice (Liu et al., 2015; DiSabato et al., 2021) with global IL-1R1 restoration (IL-1R1$^{GR/GR}$) and cell-type-specific restoration of IL-1R1 on endothelial cells (Tie2Cre-IL-1R1$^{r/r}$) or neurons (Vglut2Cre-IL-1R1$^{r/r}$) were obtained from Dr. Ning Quan's lab (Florida Atlantic University, FL). Mice were pair housed in a climate-controlled vivarium (temperature 23 ± 4C, humidity 30 ± 6%) on a 14hr/10hr light/dark cycle. All study protocols were approved by the Institutional Animal Care and Use Committee of the University of Cincinnati and performed in a facility accredited by the Association for Assessment and Accreditation of Laboratory Animal Care.

2.2. Surgeries and intra-subfornical organ IL-1RA microinfusion

Mice (n = 14/group) were anesthetized using isoflurane and implanted with guide cannulae (26-guage, cut 1.3 mm below pedestal, Plastics One) targeting the SFO (from bregma: AP −0.48 mm, DV 2.4 mm, ML 0 mm). All experimental manipulations were conducted following a one-week recovery period (see Fig. 1 for schematic). For SFO targeted delivery, injection cannulae extending 1.1 mm beyond the guide cannulae were inserted. Thirty minutes prior to CO_2 inhalation, IL-1RA (3 mg/ml; mouse recombinant IL-1RA from R&D systems cat# 480-RM-05) or vehicle (artificial cerebrospinal fluid; ACSF) was delivered in a volume of 200 nl over 2 min. The injector remained in place for 2 min following the injection to allow for diffusion into the SFO. This was the only time mice received treatment with IL-1RA or vehicle. To confirm that IL-1RA effects were specific to CO_2 inhalation, in a separate experimental cohort, IL-1RA or ACSF was administered to control mice exposed to air inhalation. Final group numbers after exclusions (surgical misses, missing cannulae) were CO_2/VEH (n = 13), CO_2/IL-1RA (n = 10), Air/VEH (n = 10) and Air/IL-1RA (n = 9).

2.3. Behavioral manipulations:

We used a recently developed paradigm that enables the assessment of passive and active defensive behaviors (freezing and rearing) to interoceptive threat, CO_2, followed by delayed effects of prior CO_2 inhalation on defensive responding to discrete exteroceptive cues (acoustic startle, foot shock contextual fear conditioning-extinction-reinstatement) (Telch et al., 2012). As noted above, mice received a single infusion of IL-1RA into the SFO 30 min prior to a single exposure to 5% CO_2 or air inhalation. To assess delayed effects of CO_2 inhalation, acoustic startle and foot shock contextual fear conditioning-extinction-reinstatement, testing was conducted one week later under ambient room air conditions (see Fig. 1 for experimental layout).

2.3.1. CO_2-inhalation paradigm—Mice were subjected to CO_2 (or breathing air) as described in previous studies by our group and others (Ziemann et al., 2009; McMurray et al., 2020; Vollmer et al., 2016; Taugher et al., 2014) using a dual vertical Plexiglas chamber

(25.5 cm × 29 cm × 28 cm per chamber). 5% CO_2 (in 21% O_2, balanced with N_2, Wright Brothers Inc., Cincinnati, OH) or breathing air (21% O_2 and <1000 ppm CO_2 balanced with N_2, Wright Brothers Inc., Cincinnati, OH) was infused in the upper chamber while the mice were placed in the lower compartment to avoid direct blowing of the gas, which is highly aversive to rodents. A flow meter with a steady infusion rate of 10 L/min was used for all animals and the concentration of CO_2 within the lower chamber was verified (5.0 ± 0.5%) by the CARBOCAP® GM70 carbon dioxide meter (GMP221 probe with accuracy specification +/−0.5%) (Vaisala, Helsinki, Finland).

Mice were acclimated to a CO_2 chamber (Day 0). The following day (Day 1), mice were returned to the chamber and exposed to air or 5% CO_2 for 10 min during which time passive (freezing) and active (rearing) behaviors were assessed. The day after CO_2 exposure animals were returned to the chamber for 5 min in the absence of CO_2. Mice were video recorded for later analysis. Freezing (complete lack of movement except for respiration) was scored using the FreezeScan software (CleverSys Inc.) and rearing (standing on hind legs with or without foreleg contact on wall) was scored by a trained observer blinded to experimental condition. CO_2-evoked freezing behavior appears to be consistent in rodents and likely represents a fear-associated defensive behavior. Rearing frequency has been reported to represent context exploratory behavior and escape motivation (GRIEBEL et al., 1996; Shansky, 2015; Biagioni et al., 2016) and was included in addition to freezing on both days to assess active and passive behaviors to threat evoked by CO_2 itself or on re-exposure to context.

2.3.2. Acoustic startle—One week following the CO_2 exposure (Fig. 1 layout), startle response to an unexpected acoustic stimulus was measured using the SR-LAB startle response system (San Diego Instruments, San Diego, CA) in standard room air as previously described with modifications (McMurray et al., 2020; Schubert et al., 2018). The enclosure was of sufficient size to restrict but not restrain the animal, as it allowed mice to turn around. The chambers were calibrated using the SR-LAB standardization unit (San Diego Instruments, San Diego, CA), prior to testing. Background noise in the chamber was maintained at 68 dB. After a 5 min acclimatization period, mice were exposed to 10 trials of 110 dB stimuli over the 68 dB background (40 ms duration; 30–38 s inter-trial interval) followed by 30 trials included randomly generated 0, 95, 100, 110, 115 and 120 db stimuli over background (40 ms duration; 30–38 s inter-trial interval). Movement inside the tube was detected by a piezoelectric accelerometer below the frame. For each trial, measurements were taken at 1 ms intervals for a response window of 150 ms following the startle stimulus using National Instruments Data Acquisition Software (San Diego Instruments, San Diego, CA). The maximum response amplitude (Vmax; mV) within the recording window was used for data.

2.3.3. Contextual fear conditioning—Mice underwent a foot shock contextual conditioning paradigm to investigate fear acquisition, conditioned fear, extinction and reinstatement in standard room air as described in previous studies (McMurray et al., 2020; Schubert et al., 2018). Operant chambers housed in sound attenuated isolation cabinets were used (CleverSys Inc.). The floors of the chambers consisted of stainless-steel grid bars that delivered scrambled electric shocks. The grid, floor trays and chamber walls

were wiped with 10% ethanol and allowed to dry completely. Mice acclimated for 5 min before receiving 3 shocks (0.5 mA, 1 sec duration, 1 min apart). Mice were returned to the chamber the next 6 days and behaviors were recorded for 5 min without shocks to measure conditioned fear (Day 2) and extinction (Days 3–7). After the first 5 min on day 7, mice received 1 reminder shock (0.5 mA, 1 sec) and remained in the chamber for 5 min to measure reinstatement of fear. Freezing behavior was scored using automated FreezeScan software (CleverSys Inc.). We also assessed post-shock rearing behaviors on acquisition and reinstatement days as a measure of an active defensive behavior. Frequency of rearing was scored by a trained observer blinded to experimental condition.

2.4. Characterization of cell-type specific expression of IL-1R1 in the SFO

We used previously developed IL-1R1 *restore* reporter mice that allow visualization of IL-1R1-expressing cells in vivo and selective expression of IL-1R1 using cell-type specific, cre-dependent promoters and amplification of tdTomato signal by a sensitive anti-RFP antibody (Liu et al., 2015; Liu et al., 2019). We used globally restored IL-1R1$^{GR/GR}$ mice that express IL-1R1 on all cell types tracked by tdTomato fluorescence, and cell-type specific reporter mice: Tie2Cre-IL-1R1$^{r/r}$ (IL-1R1 restored on endothelial cells) and Vglut2Cre-IL-1R1$^{r/r}$ (IL-1R1 restored on neurons). Previous studies suggest low or negligible expression of IL-1R1 in astrocytes and microglia (Liu et al., 2019). Brains were collected from IL to 1R1$^{GR/GR}$, Tie2Cre-IL-1R1$^{r/r}$ and Vglut2Cre-IL-1R1$^{r/r}$ mice for immunohistochemistry.

2.5. Immunohistochemistry (IHC)

For FosB and Iba1 IHCs, brain tissue was collected from mice post-behavior. Transgenic IL-1R1 reporter mice were used for detection of red fluorescent protein (RFP). Mice were perfused transcardially with 4% paraformaldehyde and processed for IHC as previously described (McMurray et al., 2020; Vollmer et al., 2016). Briefly, 30 μm coronal brain sections were cut and stored in cryoprotectant (0.1 M phosphate buffer, 30% sucrose, 1% polyvinylpyrrolidone, and 30% ethylene glycol) at −20 °C. For immunolabeling, slices were washed 5 times for 5 min (5×5 m) in PBS, incubated with 3% H_2O_2 for 10 min then washed (5×5 m) in PBS. Tissue was then incubated overnight with primary antibodies against FosB (FosB 1:20,000 Abcam cat#ab184938), ionized calcium-binding adapter molecule (Iba1; 1:1000 Synaptic Systems cat#234003) or red fluorescent protein (RFP; 1:1000 Rockland cat#600–401–379). The following day, sections were washed again (5×5 m) in PBS. For FosB staining, slices were incubated in biotinylated secondary antibody (Biotinylated Goat anti-Rb 1:400 in blocking solution; Vector Laboratories, BA-1000) for 1 h. Sections were washed (5×5 m) in PBS then incubated in avidin–biotin complex using ABC Vectastain kit, diluted 1:800 for 1 h. Following washes, sections were incubated in diaminobenzadine (DAB, Pierce, Rockford, IL) and H_2O_2 for approximately 10 m, then washed (5×5 m) in PB. Sections were mounted onto Gold Seal UltraStick microscope slides followed by dehydration in Xylene solution, then slides were cover-slipped using DPX (Sigma, 44581). For Iba1 and RFP immunofluorescence staining, sections were incubated in Cy3 secondary antibody (Cy3 anti-Rb 1:500 Jackson, cat#711–165–152) for 1 h, then washed (5×5 m) in PB, mounted, and cover-slipped using Gelvatol (Sigma-Aldrich cat#10981–100 ml).

To maintain consistency between samples for each stain, all sections were processed for immunostaining in the same run at the same time.

2.6. Image analysis and cell counting

Immunolabeled sections were mounted and imaged at 5x using an AxioImager ZI microscope (Axiocam MRm camera and AxioVision Release 4.6 software; Zeiss). For FosB, regions were selected for full quantification and analysis based on previous CO_2 studies (McMurray et al., 2020; McMurray et al., 2019), their role in threat responding and fear regulation, or if preliminary immunostaining assessments suggested differences between experimental groups. Quantified areas included the medial prefrontal cortex (mPFC) including both the infralimbic (IL, AP 1.98 to 1.34) and prelimbic (PL, AP 1.98 to 1.42) cortices, nuclei of the amygdala including basolateral, central lateral, central medial nuclei and intercalated cells of the amygdala (BLA, CeA, ITC; AP −0.94 to −2.06), the dorsolateral and ventrolateral/lateral regions of the periaqueductal gray (dl PAG, vl/l PAG: AP −3.52 to −4.84) and the dorsal dentate gyrus of the hippocampus (dDG, AP −1.34 to −2.92). Regions were delineated using characteristics of each nucleus based on the atlas of Paxinos and Watson (Paxinos and Watson, 1998). At least 3–4 images per region of interest per hemisphere were collected for each mouse. FosB immune-positive cells were counted using the Image-J “cell counter” tool (ImageJ, NIH) by an investigator blind to experimental group. A standard threshold level and minimum pixel size within the analyze particle function were determined for each region. Due to the dense FosB expression within DG, the optical density of the FosB stain was quantified instead of individual cell counts using ImageJ. Pixel values were converted to optical density by creating a Rodbard calibration curve. Optical density was reported as the value obtained from subtracting a background measure of the slice from the outlined area of interest within DG. For morphological alterations in microglia within the SFO (AP −0.10 to −0.80), we analyzed soma perimeter of Iba-1 positive cells using the ImageJ software tool “Freehand line” and recorded using the “Analyze and Measure” option as done previously (Vollmer et al., 2016). To confirm whether treatment effects on SFO microglial alterations were specific, we also assessed Iba-1 positive cells in areas adjacent to the SFO: the rostral dentate gyrus of the hippocampus (HPC; AP −0.94 to −1.22), and paraventricular nucleus of the thalamus (PVT; AP −0.22 to −0.82). Cell counts for each section were averaged for each animal and individual means averaged to derive group means.

2.7. Correlational analysis of behavior and brain regional activation

To explore the relationship between behaviors and brain regional activity, pairwise Pearson correlation coefficients were determined as previously described (McMurray et al., 2020; McMurray et al., 2019) for FosB + cell counts and percent freezing during Air/CO_2 inhalation (Day 1), Air/CO_2 context re-exposure (Day 2), footshock contextual fear conditioning acquisition (average freezing across all 3 shocks), conditioned fear, early extinction (average of extinction days 1–2), later extinction (average of extinction days 3–5), and reinstatement. Correlational analysis was limited to regions with significant treatment and/or inhalation effects for FosB + cell counts: infralimbic cortex (IL), intercalated cells of the amygdala (ITCs), basolateral amygdala and the dorsolateral and ventrolateral/lateral regions of the periaqueductal gray (dl PAG, vl/l PAG).

2.8. Quantification of IL-1β and IL-1R1 expression

In a separate experiment, mice were exposed to air and CO_2 inhalation for conducting real time quantitative PCR (RTqPCR) analysis in peripheral blood mononuclear cells and SFO tissues in a time dependent manner (Fig. 5, schematics). Submandibular blood was collected from mice a week prior to CO_2 (n = 16) or air (n = 8) inhalation and immediately following inhalation for pre- and post- inhalation assessment of IL-1β and IL-1R1 expression. To enrich for mononuclear cells, blood samples were layered into BD Vacutainer® CPT Mononuclear Cell Preparation Tubes (Becton, Dickinson and Company, New Jersey) as described before by us (Strawn et al., 2018) and centrifuged for 20 min at 1500 × g at room temperature. The buffy coat was aspirated, aliquoted and centrifuged to yield a cell pellet. SFO tissue was collected and analyzed as described in (Winter et al., 2019), with modifications. Separate groups of mice were exposed to air (n = 8) or CO_2 (n = 8) and brains were collected immediately (0), 4, 8 or 24 h post inhalation. Brains were flash frozen with isopentane and stored at −80 °C until being sectioned. Tissue punches were taken from frozen SFO slices (AP −0.10 to −0.80) on a cryostat using a 0.5 mm internal diameter tissue punch. For blood and brain samples, total RNA was isolated using a Qiagen RNeasy kit. cDNA was generated using Invitrogen SuperScript IV First-Strand Synthesis System and quantitative real-time PCR was conducted on a Taqman 7900 using PowerUp SYBR Green Master Mix (A25742) using primers for IL-1β (FWD: CAGGCTCCGAGATGAACAAC, REV: GGTGGAGAGCTTTCAGCTCATAT), IL-1R1 (FWD: CCTCACGGCTACAATTGTATGC, REV: CAAACTGTCCCTCCAAGACC), and GAPDH (FWD: GAAGGTCGGTGTGAACGGATTTGGC, REV: GATGGGCTTCCCGTTGATGACAAGC) (Liu et al., 2015; Bollinger et al., 2020). Fold induction was calculated using the delta-delta ct method as described previously (Strawn et al., 2018).

2.9. Statistical analysis

Data are represented as means ± standard error and inferential statistical analyses included students' unpaired *t*-test, two-way ANOVA or three-way repeated measures ANOVA as appropriate. Welch's corrections were applied when distributions had unequal variance. Non-parametric Mann-Whitney tests were applied to distributions failing normality as determined by the Kolmogorov-Smirnov test. For *post hoc* analyses, Benjamini, Krieger and Yekutieli tests were applied which correct for multiple comparisons. Pearson's correlation coefficients were calculated to test associations between two outcomes of interest (i.e., FosB + cell counts and freezing). Grubbs' tests were performed to determine and remove any outliers (1 statistical outlier was removed from the analyses). Results were considered statistically significant at the $p < 0.05$ level and statistical analyses were performed in *Prism*, version 8 (GraphPad Software, Inc., La Jolla, CA).

3. Results

3.1. SFO-IL-1R1 regulates spontaneous active and passive defensive behaviors to CO_2-Inhalation:

We assessed freezing and rearing as a measure of passive and active defensive behaviors, respectively. As shown in Fig. 2A, IL-1RA treatment significantly reduced freezing ($F_{(1,38)}$

= 7.796, p = 0.008). Post hoc tests revealed significantly increased freezing in CO_2-exposed, SFO-vehicle treated mice compared to air-exposed, SFO-IL-1RA ($p < 0.05$) and CO_2-exposed, SFO-IL-1RA ($p < 0.05$) treated mice, as well as a near significant increase compared to Air-exposed, SFO-vehicle treated mice ($p = 0.053$). No significant differences were noted within air-exposed groups. For CO_2-evoked rearing behavior, there was a significant treatment × inhalation interaction ($F_{(1,34)} = 4.264$, $p = 0.047$, Fig. 2B. Post-hoc analysis revealed that SFO-IL-1RA treatment attenuated the reduction in rearing during CO_2 inhalation (CO_2/VEH vs CO_2/IL-1RA $p < 0.05$). Consistent with CO_2-associated contextual freezing reported by us in previous studies (Vollmer et al., 2016; McMurray et al., 2019), re-exposure to inhalation context elicited higher freezing in CO_2 exposed mice ($F_{(1,37)} = 10.25$, $p < 0.01$, Fig. 2C and reduced rearing ($F_{(1,34)} = 3.499$, $p = 0.07$. Fig. 2D; however, SFO-IL-1RA infusion had no significant effect on freezing or rearing.

3.2. SFO-IL-1R1 mediates delayed effects of CO_2 on threat responding to exteroceptive cues: Modulation of contextual fear conditioning, extinction and reinstatement

As reported in previous studies by our group (McMurray et al., 2020), we assessed delayed effects of CO_2 on behavioral responding to two discrete exteroceptive stimuli differing in modality and intensity: acoustic startle and contextual fear conditioning. As shown in Supplemental Fig. 1, on exposure to a variable range of acoustic stimuli one week following inhalation, a significant overall effect of decibel on startle amplitude was observed ($F_{(5,175)} = 107.5$, $p < 0.0001$). However, no significant effects of treatment, inhalation or inhalation × treatment interaction were observed.

The day after acoustic startle, mice underwent a foot shock contextual fear conditioning paradigm. On fear acquisition day, there was a significant effect of time ($F_{(3,114)} = 121.7$, $p < 0.0001$, Fig. 3A and a trending interaction between inhalation and treatment ($F_{(1,38)} = 3.734$, $p = 0.061$). Post hoc tests revealed reduced freezing in previously CO_2-exposed, SFO-IL-1RA treated mice compared to Air-exposed, SFO-vehicle treated mice during habituation ($p < 0.05$) and compared to CO_2-exposed, SFO-vehicle treated mice after the 2nd and 3rd shocks ($p < 0.05$). Interestingly, this was accompanied by significantly altered rearing during the post-shock period (time × inhalation: $F_{(3,111)} = 2.777$, $p = 0.045$; inhalation × treatment: $F_{(1,37)} = 6.900$, $p = 0.013$; time: $F_{(3,111)} = 43.86p < 0.001$; Fig. 3B. Previously CO_2-exposed, SFO-IL-1RA treated mice showed significantly higher rearing frequency compared to CO_2-exposed, SFO-vehicle treated mice after shock 2 ($p < 0.05$) and compared to Air-exposed, SFO-vehicle treated mice after the 2nd and 3rd shocks. Importantly, this effect was CO_2-specific, as SFO-IL-1RA did not alter rearing in groups previously exposed to air. Together, these data suggest differences in defensive coping behaviors during fear acquisition. On context exposure 24 h post acquisition (Fig. 3C), there was a significant treatment × inhalation interaction ($F_{(1,38)} = 4.110$, $p = 0.0497$) and a treatment effect that did not reach statistical significance ($F_{(1,38)} = 3.303$, $p = 0.077$). Post hoc tests revealed prior IL-1RA treatment significantly reduced freezing (conditioned fear) only in CO_2-exposed mice ($p < 0.05$). During extinction training (Days 3–6, Fig. 3D there were significant overall treatment and time effects (Treatment: $F_{(1,37)} = 5.064$; $p = 0.031$; Time: $F_{(3,111)} = 36.13$, $p < 0.0001$). Post hoc tests revealed significantly higher freezing in CO_2-exposed, SFO-vehicle treated mice compared to CO_2-exposed, SFO-IL-1RA treated mice during extinction days

1 and 3 (E1: $p < 0.05$, E3: $p < 0.01$), compared to Air-exposed, SFO vehicle treated mice during extinction day 3 ($p < 0.01$) and compared to Air-exposed, SFO-IL-1RA treated mice during extinction days 2, 3 and 4 (E2: $p < 0.05$, E3: $p < 0.01$, E4: $p < 0.01$). To assess return of fear we performed fear reinstatement. Freezing (Fig. 3E) and rearing (Fig. 3F) were measured before (pre-) and post- exposure to a single reminder shock. For freezing, there was a significant main effect of inhalation ($F_{(1,37)} = 9.664$, $p = 0.004$) and time ($F_{(1,37)} = 8.097$, $p = 0.007$), as well as, a nearly significant main effect of treatment ($F_{(1,37)} = 3.957$, $p = 0.054$). There was also a significant time × treatment interaction of ($F_{(1,37)} = 11.77$, $p = 0.002$). Post-hoc analysis revealed significantly higher freezing in prior CO_2-exposed SFO-vehicle treated mice compared to Air-exposed, SFO-vehicle and Air-exposed, SFO-IL-1RA treated mice group at both the pre (CO_2/VEH vs Air/VEH: $p < 0.05$; vs Air/IL-1RA: $p < 0.01$) and post shock time points (CO_2/VEH vs Air/VEH: $p < 0.01$; vs Air/IL-1RA: $p < 0.01$). Additionally, prior SFO-IL-1RA treatment in CO_2-exposed mice reduced freezing compared to CO_2-exposed SFO-vehicle treated mice during the post shock period ($p < 0.01$). For rearing, there was a significant overall effect of inhalation ($F_{(1,31)} = 2.34$, $p = 0.01$) and trending inhalation × treatment ($F_{(1,31)} = 3.326$, $p = 0.078$) and treatment × time ($F_{(1,31)} = 2.979$, $p = 0.094$) interactions. Post hoc tests revealed significantly reduced rearing frequency in previously CO_2-exposed, SFO-vehicle treated mice compared to Air-exposed, SFO-vehicle treated mice during both the pre- ($p < 0.05$) and post-shock ($p < 0.01$) periods. Collectively, these data show that SFO-IL-1R1 signaling mediates delayed effects of CO_2 on contextual fear conditioning, extinction and reinstatement by altering defensive threat responding that favors active versus passive behaviors.

3.3. Engagement of cortico-amygdala-PAG subregions in SFO-IL-1R1 modulation of CO_2-associated fear

To identify brain regions that may contribute to SFO IL-1R1 mediated behavioral regulation, we conducted post-behavioral assessment of FosB, a surrogate marker for sustained neuronal activation. Regions associated with threat responding and regulation of defensive behaviors were investigated. Analysis of the infralimbic cortex (IL) subdivision of the medial prefrontal cortex (Fig. 4A) revealed a significant overall effect of treatment ($F_{(1,36)} = 5.615$, $p = 0.023$) and a treatment × inhalation interaction ($F_{(1,36)} = 4.175$, $p = 0.048$). Post hoc tests revealed prior CO_2-exposure significantly reduced FosB + cells within SFO-vehicle treated mice (CO_2/VEH) as compared to Air/VEH ($p < 0.05$) and Air/IL-1RA ($p < 0.05$). SFO-IL-1RA treatment in CO_2-exposed mice restored FosB + cell counts (CO_2/VEH vs CO_2/IL-1RA $p < 0.01$) while no effect was observed within Air-exposed groups. Within the prelimbic (PL) cortex (Fig. 4B), no significant effect of inhalation, treatment or treatment × inhalation interaction was observed. Subregion-specific alterations were also observed within the amygdala. A significant overall effect of treatment ($F_{(1,37)} = 5.839$, $p = 0.021$) and a trend for inhalation × treatment interaction ($F_{(1,37)} = 3.111$, $p = 0.086$) was observed within the intercalated cell cluster (ITC, Fig. 4C). Post hoc tests revealed prior CO_2-exposure significantly reduced FosB + cells within SFO-vehicle treated mice (Air/VEH vs CO_2/VEH: $p < 0.05$); Air/IL-1RA vs CO_2/VEH: $p < 0.05$). SFO-IL-1RA treatment in CO_2-exposed mice restored FosB + cell counts (CO_2/VEH vs CO_2/IL-1RA: $p < 0.05$), however no significant differences were observed between air-exposed mice. Within the basolateral amygdala (BLA), CO_2 inhalation significantly increased FosB +

cell counts (overall inhalation effect: $F_{(1,38)} = 25.72$, $p < 0.0001$, Fig. 4D, however, there was no treatment or treatment × inhalation interaction effect. No significant effects were observed within the central amygdala (CeA) subdivision (Fig. 4E). Within the dorsolateral periaqueductal gray (dl PAG, Fig. 4F), IL-1RA treatment significantly reduced FosB + cell counts (overall treatment effect: $F_{(1,35)} = 4.463$, $p = 0.042$), however, there were no effects of inhalation, inhalation × treatment interaction and no individual group differences. Within the ventrolateral/lateral periaqueductal gray (vl/l PAG, Fig. 4G), CO_2 inhalation significantly increased FosB + cell counts (overall inhalation effect: $F_{(1,35)} = 7.664$, $p = 0.009$). Post hoc tests revealed prior CO_2-exposure significantly increased FosB + cells in SFO-vehicle treated mice (Air/VEH vs CO_2/VEH: $p < 0.05$); Air/IL-1RA vs CO_2/VEH: $p < 0.05$), but no significant differences were evident from the CO_2/IL-1RA group. Lastly, there were no significant group differences in FosB cell counts within the hippocampal dentate gyrus (DG, Fig. 4H).

To investigate the association between observed behaviors and neural activation, we correlated FosB + cell counts with freezing during different phases of the Air/CO_2 inhalation and footshock contextual fear conditioning paradigms (Table 1). Analysis was limited to regions with treatment and/or inhalation effects. For the Air/CO_2 paradigm, a trending negative correlation was observed between IL FosB + cell counts and Air/CO_2 freezing (Pearson $r = -0.277$, $p = 0.088$) and with context re-exposure freezing the following day (Pearson $r = -0.268$, $p = 0.099$), while the dlPAG FosB + counts showed a trending positive correlation with Air/CO_2 freezing (Pearson $r = 0.302$, $p = 0.069$). In the footshock contextual fear conditioning paradigm, freezing during late extinction (days 3–5) and reinstatement testing showed strong associations with regional FosB counts. While IL and ITC FosB + cell counts were significantly negatively correlated with freezing (IL: Pearson $r = -0.382$, $p = 0.016$; ITC: Pearson $r = -0.438$, $p = 0.005$), the vl/l PAG was significantly positively correlated (Pearson $r = 0.346$, $p = 0.034$, and dl PAG showed a trending positive correlation (Pearson $r = 0.289$, $p = 0.083$). Similarly, for reinstatement freezing, IL and ITC FosB + cell counts were significantly negatively correlated (IL: Pearson $r = -0.534$, $p = 0.001$; ITC: Pearson $r = -0.464$, $p = 0.003$), while dl and vl/l PAG showed positive correlations (dl PAG: Pearson $r = 0.310$, $p = 0.061$; vl/l PAG: Pearson $r = 0.300$, $p = 0.067$. Other testing phases during fear conditioning also showed region-specific associations: fear acquisition freezing (ITC FosB + counts Pearson $r = -0.289$, $p = 0.075$), conditioned fear (dl PAG Pearson $r = 0.284$, $p = 0.089$) and early extinction (days 1–2) (dl PAG: Pearson $r = 0.295$, $p = 0.075$). No correlations were observed between BLA FosB + cell counts and freezing behaviors (data not shown).

3.4. Endothelial localization of IL-1R1 within the SFO and CO_2 induced regulation of IL-1β/IL-1R1 expression

To further understand IL-1R1 contributions, we characterized cell-type specific expression of the receptor within the SFO. To avoid artifacts in the detection of IL-1R1, we used IL-1R1$^{GR/GR}$ mice, that have an IRES site followed by tdTomato sequence inserted in exon 11 of IL-1R1 gene (Liu et al., 2015), to track global expression of IL-1R1. As shown in Fig. 5A, intense tdTomato fluorescence was observed in blood vessels within the SFO in IL-1R1$^{GR/GR}$ mice. Examination of Tie2Cre-IL-1R1$^{r/r}$ mice that have endothelial-

specific expression of IL-1R1 confirmed SFO slices expressed intense IL-1R1 dependent tdTomato fluorescence in endothelial cells within blood vessels similar to the tdTomato distribution in global restore mice (Fig. 5B). In comparison, no IL-1R1 dependent tdTomato signal was evident in SFO slices from Vglut2Cre-IL-1R1$^{r/r}$ mice that have neuron-specific expression of IL-1R1 (Fig. 5C), while hippocampal dentate gyrus neurons showed high IL-1R1 expression dependent tdTomato (Fig. 5D).

Given the association of IL-1R1 with endothelial cells within blood vessels, we investigated CO_2– evoked regulation of IL-1β/IL-1R1 expression in blood monocytes that have been identified previously as a peripheral source of IL-1β in periphery-brain signaling in inflammatory and stress states (McKim et al., 2018; Nakamori et al., 1995). As shown in Fig. 5E, baseline (pre-CO_2) monocytic expression of IL-1β was not different between air and CO_2 groups (IL-1β: non-parametric Mann-Whitney U: 25, p = 0.2463); However, exposure to CO_2 inhalation triggered a significant increase in IL-1β expression (Welch-corrected t = 2.664, df = 10.30, p = 0.023, Fig. 5E). No significant group differences were observed in IL-1R1 expression (Fig. 5F) at either pre-CO_2 (non-parametric Mann-Whitney U: 37p = 0.5356) or post CO_2 time points (t = 0.6954, df = 20, p = 0.49). We also measured regulation of IL-1β/IL-1R1 expression in tissue punches from the SFO collected post air/CO_2 inhalation at 0, 4 h, 8 h and 24 h. As shown in Fig. 5G, a significant decrease in IL-1β expression was observed at the 8 h timepoint (*t* test, $t_9 = 3.269$, p = 0.009) in the CO_2-exposed group. No significant differences were observed at any other time points (Fig. 5H). Similarly, SFO IL-1R1 expression showed a marked reduction at the 8 h time point but did not reach statistical significance (Welch-corrected *t*-test, $t_9 = 2.104$, p = 0.08). No significant differences were observed at any other time points.

Based on our previous data showing microglial involvement in CO_2-evoked fear (Vollmer et al., 2016), we also assessed the effects of SFO IL-1RA infusion on morphological activation of microglia in air and CO_2-exposed mice post behavior (Fig. 5I and J). There were significant overall effects of inhalation ($F_{(1,38)} = 18.80$, p = 0.0001) and treatment ($F_{(1,38)} = 6.500$, p = 0.015), as well as a significant interaction of treatment and inhalation ($F_{(1,38)} = 22.21$, p < 0.0001). Post hoc analysis revealed significantly increased microglial soma perimeter in CO_2/Veh mice compared with Air/Veh mice (p < 0.0001). Importantly, SFO IL-1RA treatment attenuated the effect of CO_2 on microglial soma perimeter (p < 0.0001) but had no effect within Air-exposed mice.

To determine the regional specificity of the effect of SFO IL-1RA treatment on CO_2-evoked microglial effects, we also measured microglial soma perimeter in the paraventricular thalamus and dentate gyrus of the hippocampus (HPC). These areas are fear-regulatory regions in close proximity to the SFO infusion site and located either directly ventral to the SFO (PVT; directly across the 3rd ventricle) or immediately posterior to the SFO (HPC) and could have been affected by leakage of IL-1RA out of the SFO. However, there was no effect of IL-1RA treatment within CO_2-exposed mice in either the HPC (Supplemental Fig. 2a) or PVT (Supplemental Fig. 2b).

4. Discussion

Our data reveals a unique and unprecedented role of IL-1R1 receptor within the SFO as a regulator of fear-associated threat responding. SFO-targeted antagonism of IL-1R1 regulated not only spontaneous defensive behaviors to CO_2 inhalation, a PD and PTSD relevant interoceptive stimulus, but also impacted delayed effects of prior CO_2 on exteroceptive stressors: contextual fear conditioning, extinction, and reinstatement, as well as neuronal activation within fear regulatory areas. Furthermore, endothelial localization of IL-1R1 within the SFO and CO_2-mediated alterations in monocyte IL-1β expression suggest an engagement of body to brain signaling mechanisms in CO_2-modulation of spontaneous and conditioned fear.

The current study extends our previous findings on the role of neuroimmune signaling via IL-1β/IL-1R1 in CO_2 inhalation evoked freezing (Vollmer et al., 2016). CO_2, a widely studied interoceptive stimulus, produces an imminent danger to survival resulting in intense fear, autonomic, and respiratory responses that can evoke panic attacks in vulnerable individuals such as those with panic disorder and PTSD (Gorman et al., 1994; Papp et al., 1993; Muhtz et al., 2012; Vollmer et al., 2015; Kellner et al., 2018). In the extracellular space, CO_2 combines with water to produce protons, leading to systemic acidosis (Magnotta et al., 2012; Loeschcke, 1982), an internal threat to homeostasis that impacts behavior and physiology. Previously, we observed CO_2-evoked activation of SFO neurons that was attenuated by IL-1RA infusion using slice electrophysiology, suggesting a potential role of SFO IL-1R1 in regulating CO_2-associated fear. Other studies have reported effects of IL-1β/IL-1R1 signaling on a wide range of behaviors relevant to anxiety, sickness and depression, as well as, learning and memory (Goshen et al., n.d; Rachal Pugh et al., 2001; McKim et al., 2018; DiSabato et al., 2021; Dantzer, 2009; Koo and Duman, 2009). Evidence from genetic and pharmacological manipulations suggests that optimal IL-1R1 signaling is required for fear learning and memory (Goshen et al., n.d; Koo and Duman, 2009), particularly hippocampal-dependent contextual fear memory (Goshen et al., n.d). Recent work has also shown the relevance of hippocampal IL-1R1 in stress-enhanced fear learning (Jones et al., 2015; Jones et al., 2018), as well as social withdrawal and cognitive deficits (DiSabato et al., 2021). Our data provides evidence that in addition to regulating exteroceptive stress effects through traditional fear-regulatory brain areas, IL-1β/IL-1R1 signaling via the sensory circumventricular organ, SFO, modulates acute fear responses to interoceptive stressor, CO_2, and potentiates fear to subsequent exteroceptive threats. Importantly, SFO targeted IL-1RA treatment had no effect on traditional fear regulatory regions located in close proximity to the SFO like the hippocampus (immediately posterior) and the paraventricular nucleus of the thalamus (across the 3rd ventricle, immediately ventral) within this model. This suggests these effects are unlikely to be the result of IL-1RA leakage outside of the SFO during the infusion.

The SFO represents an integrative site with a compromised blood-brain barrier, permitting access to systemic and CNS compartments for maintenance of homeostasis (Johnson and Gross, 1993). The SFO has largely been studied as a homeostatic sensory locus regulating hydro-mineral balance, cardiovascular responses, energy balance, immune responses, and reproduction (Johnson and Gross, 1993; McKinley et al., 2003; McKinley et al., 1998).

The SFO can effectively sense fluctuations in osmolarity, volume and pressure of the circulation to drive motivated behaviors such as drinking, cardiovascular regulation, and food intake (McKinley et al., 2019; Ferguson, 2014; Mimee et al., 2013). Activation of the SFO by unpleasant homeostatic states such as dehydration or hyperosmolality produces a negative valence signal that promotes adaptive behaviors such as water intake to normalize homeostatic balance. However, the role of CVOs such as the SFO as merely passive sensors of homeostatic milieu has been changing and recent work reported that the SFO can enable dynamic regulation of anticipatory behaviors related to thirst and satiety (Zimmerman et al., 2016; Hsu et al., 2020). Our observations suggest that in addition to regulating motivated behaviors such as drinking and food intake, the SFO regulates defensive responding to interoceptive stimuli that generate fear and panic. It is possible that physiological responses such as altered breathing and cardiovascular activation by CO_2 inhalation contribute to SFO-IL-1R1 mediated regulation of defensive behaviors. In this regard, the SFO regulates blood pressure (Smith and Ferguson, 2010) as well as respiration (Ferguson et al., 1989), and previous studies reported IL1β-IL1R signaling mediated cardiovascular activation via the SFO (Wei et al., 2013). It would be important to tease out the contribution of respiratory and cardiovascular responses in SFO-IL-1R1 regulation of defensive behaviors.

Interestingly, in addition to modulating spontaneous defensive behaviors during CO_2 inhalation, SFO IL-1RA treatment regulated the effects of prior CO_2 inhalation on contextual fear memory a week later. Relevance of homeostatic perturbations and interoceptive signals in shaping behavior has long been recognized (Damasio and Carvalho, 2013), and there is significant interest in how interoceptive processes integrate with emotional regulation and mental health (Khalsa et al., 2018). In this regard, emotional reactivity to CO_2 at pre-deployment was associated with increased posttraumatic-stress symptoms to subsequent war-zone stressors (Telch et al., 2012). Previously, we reported an association of a prior CO_2 exposure with enhanced fear conditioning and compromised extinction in mice (McMurray et al., 2020), suggesting that previous interoceptive experiences regulate long term fear behaviors. Our current data support a role of SFO IL-1R signaling in mediating this phenomenon. As compared to the CO_2-exposed vehicle group, SFO IL-1RA-treated mice elicited reduced freezing during acquisition, conditioned fear and extinction phases of a contextual conditioning paradigm. Furthermore, increased post-shock rearing frequency in SFO-IL-1RA mice during acquisition and reinstatement may be suggestive of altered defensive threat responding, favoring active rather than passive behaviors. Although it is difficult to extrapolate the translational relevance of active versus passive behavioral strategies, previous evidence supports an association of active coping behavioral strategies with reduced incidence of PTSD (Olff et al., 2005). Since SFO IL-1RA treatment had no such effects in air exposed mice, attenuated freezing and increased rearing are likely associated with delayed effects on CO_2 rather than regulation of fear learning and memory as previously reported for IL-1β/IL-1R1 blockers (Goshen et al., n.d). The lack of significant treatment effects on acoustic startle and pre-shock habituation freezing is consistent with our previous study (McMurray et al., 2020), suggesting that prior CO_2 exposure (and IL-1R1 signaling) does not result in generalized fear sensitization, but that effects may be dependent on the modality and intensity of aversive experiences. SFO IL-1R1 modulation of delayed CO_2-potentiated fear memory and extinction deficits appears to be

selective as no effects were observed on contextual freezing to CO_2 context 24 h post inhalation. Contextual freezing to the CO_2 context could also depend on SFO-independent circuits and discrete downstream mechanisms engaged by CO_2 -evoked acidosis such as the acid sensing ion channels (ASICs) in the amygdala (Ziemann et al., 2009). It would be important to determine whether IL-1R1 in traditional fear regulatory nodes such as the amygdala and hippocampus can regulate CO_2-associated fear memory. IL-1R1 receptors within these areas have been reported to regulate fear (Jones et al., 2015; Chiu et al., 2012; Goshen et al., n.d; Jones et al., 2018; Rachal Pugh et al., 2001), however, to our knowledge they have not been implicated in CO_2-evoked behaviors.

Our post behavior FosB data suggest potential brain regions that integrate in SFO IL-1R1 mediated attenuation of CO_2-evoked fear and effects on contextual fear conditioning. Significant differences were observed in subregions within the amygdala, prefrontal cortex and periaqueductal gray (PAG); areas that process unconditioned and conditioned defensive threat responding (Fanselow, 1994; Paré et al., 2004; Misslin, 2003; Maddox et al., 2019). Previous studies have reported cortical-amygdala interactions in regulating fear learning and extinction (Marek et al., 2013; Strobel et al., 2015). Reduced activation in the IL and ITCs has been associated with increased fear and compromised extinction (Likhtik et al., 2008; Sierra-Mercado et al., 2011; Do-Monte et al., 2015). Consistent with their “high fear” phenotype, CO_2-vehicle treated mice showed a reduction in $FosB^{+ve}$ cells within the IL cortex and amygdala ITCs, an effect normalized by SFO-IL-1RA treatment, as well as increased FosB in the basolateral amygdala. Lack of an IL-1RA effect in the BLA may suggest that SFO modulation of CO_2-associated fear may recruit alternative fear circuits. An absence of significant alterations within the central amygdala and the hippocampus in the current study is surprising; given our previous results showing recruitment of these areas in CO_2-associated fear conditioning (McMurray et al., 2020). This could be attributed to different experimental layouts, as the current study involved surgeries, handling, and drug manipulations while the previous study was performed in naïve animals. Also, the temporal layout of the current study may not have captured the dynamics of FosB expression in these regions at earlier time points. Treatment and inhalation associated FosB alterations were also evident within the dorsolateral and ventrolateral subdivisions of the PAG, suggesting their engagement in observed behavioral effects. In response to threats that predict danger, the vlPAG engages passive freezing behavior, while the dlPAG controls active escape (Gross and Canteras, 2012). Previous studies by us and others reported CO_2-evoked activation of neurons within these subdivisions (McMurray et al., 2019; Johnson et al., 2005). Consistent with activation patterns observed here, the PAG is well connected to the amygdala and PFC (Fanselow, 1994; Floyd et al., 2000; Rizvi et al., 1991) and integrates with interoceptive sites for threat perception and responding (Faull et al., 2019). Disrupted PAG functional connectivity and stronger PAG-mediated engagement of cortical networks has been reported in PTSD patients exposed to trauma-related stimuli (Terpou et al., 2020; Harricharan et al., 2016; Webb et al., 2020) and stronger PAG-cortical connectivity prospectively predicts PTSD. Our FosB-behavior correlational analysis showing inverse associations for IL and ITCs and positive correlations for PAG subdivisions with extinction-reinstatement freezing also support integration of these areas in SFO regulation of fear. Collectively, these observations suggest that homeostatic loci such as the SFO engage

traditional PTSD-relevant emotion and fear regulatory networks, highlighting a crosstalk and integration of interoceptive-exteroceptive circuits. Furthermore, the ability of IL-1RA to impact neuronal activation within these regions bears therapeutic potential. Notably, no differences in either neuronal or microglial activation within the hippocampus suggests that in contrast to exteroceptive threat associated fear (Jones et al., 2015; Jones et al., 2018), IL-1R1 participation in signaling interoceptive threat-evoked fear may not recruit hippocampal mechanisms.

IL-1β/IL-1R1 expression data provides insight into potential mechanisms by which SFO IL-1R1 mediates effects of CO_2 inhalation on behavior. A significant increase in post-CO_2 IL-1β expression in blood monocytes, but not the SFO, suggests that peripheral immune cells are a likely source of IL-1β. Given the localization of IL-1R1 on endothelial cells within the SFO, our data suggests interactions between IL and 1β producing monocytes with SFO endothelial IL-1R1 in mediating CO_2 responses. A post-CO_2 reduction in SFO IL-1β and IL-1R1 expression at 8 h suggests delayed compensatory, adaptive changes in IL-1β/IL-1R1 signaling, an effect that warrants further investigation. A recent study reported recruitment of IL-1β- producing monocytes to brain endothelium in mediating social stress-induced anxiety (McKim et al., 2018). In that study, exposure to repeated cycles of social defeat caused the release of activated IL-1β-producing monocytes that are recruited to and interact with brain endothelial IL-1R1, an effect facilitated by microglia. In a previous study we reported CO_2-evoked activation of SFO microglia via acid sensor T cell death associated gene-8 receptor (TDAG8) (Vollmer et al., 2016), that temporally overlaps with increased monocyte IL-1β expression observed in the current study. Interestingly, CO_2-acidosis sensor TDAG8 is expressed in peripheral monocytes (KYAW et al., 1998) and previously we reported increased monocytic TDAG8 expression in panic disorder patients (Strawn et al., 2018). Blockade of microglial activation using non-selective agent minocycline attenuated CO_2-evoked freezing (Vollmer et al., 2016). Collectively, these data suggest a role of microglia in facilitating CO_2 -evoked fear possibly via monocyte IL-1β endothelial IL-1R1 interactions. Furthermore, IL-1RA attenuated morphological activation of SFO, but not hippocampus or paraventricular nucleus of the thalamus microglia in CO_2, but not air mice post behavior, suggesting persistence and specificity of microglial changes within the SFO. Our data synchronize with other studies reporting peripheral monocyte-endothelial-microglia interplay in mediating IL-1β-mediated responses in the brain (Liu et al., 2019; Zhu et al., 2019). Previous data, in conjunction with our findings, suggest a role of endothelial IL-1R1 in facilitating adaptive behaviors to aversive states. Mechanisms by which SFO endothelial IL-1R1 signaling regulates fear behavior need more investigation. Recent data from our group indicate a potential involvement of renin angiotensin system (RAS) mediators, angiotensin converting enzyme (ACE) and angiotensin type 1 receptor (AT1R) (Winter et al., 2019). Exposure to CO_2 upregulates SFO ACE and AT1R expression and AT1R antagonist losartan attenuated CO_2-evoked freezing (Winter et al., 2019). Enriched ACE expression has been reported in endothelial cells (Costerousse et al., 1992) and preliminary observations in our lab indicate colocalization of ACE and endothelial IL-1R1 within the SFO (unpublished observations). Future studies are required to tease out periphery-SFO communication links and downstream effectors in SFO IL-1R mediated regulation of CO_2-associated fear. Lastly, the current study focused exclusively

on male mice, however, given previous evidence reporting high reactivity to CO_2 inhalation and high PTSD prevalence in females (Shansky, 2015; Kelly et al., 2006), future studies are warranted in female mice.

5. Implications and conclusion

There is a growing interest in understanding the association of altered internal homeostatic state and regulation of emotional behaviors. A role of humoral neuroimmune pathways in "body to brain" signaling and interoception has been recognized (Quadt et al., 2018). Here, we highlight a role of endothelial IL-1R1 signaling within the SFO in regulating defensive behaviors to interoceptive threat, CO_2. Further, these data point to a novel role for SFO neuroimmune signaling in driving potentiated fear responding to later exteroceptive threats that may be relevant to understanding fear-associated disorders like PTSD. This mechanism may work in concert with other CO_2 targets, such as the ASICs in the amygdala (Ziemann et al., 2009). The existence of a homeostatic threat detection system that is distinct from traditional psychogenic fear and stress modulatory pathways may be relevant to the observed fear and panic observed in Urbach-Wiethe patients with damaged amygdala (Feinstein et al., 2013). Future studies on SFO modulation of cortico-amygdala fear circuits can provide information on the synchronization of interoceptive-exteroceptive pathways in the brain. Finally, ready access of the SFO to peripheral milieu provides opportunities for effective therapeutic targeting.

In conclusion, we report subfornical organ IL-1R1 signaling as a novel, "bottom-up" mechanism regulating threat appraisal and defensive behaviors of relevance to fear-related pathologies.

Supplementary Material

Refer to Web version on PubMed Central for supplementary material.

Acknowledgements

We would like to thank Dr. Ning Quan for IL-1R1 transgenic restore mice and Xiaoyu Liu for helpful discussions.

Funding and Disclosure

This work was supported by VA Merit Grants 2I0–1BX001075 and I01-BX001075 to RS. Support is also acknowledged from postdoctoral training award F32MH117913 (KMJM). AW would like to acknowledge support from a T32 pre-doctoral training program in Neuroscience grant (T32 NS 007453). The content is solely the responsibility of the authors and does not necessarily represent the official views of the NIH. The authors declare no competing interests.

References

Pfeifer G, Garfinkel SN, Gould van Praag CD, Sahota K, Betka S, Critchley HD, 2017. Feedback from the heart: Emotional learning and memory is controlled by cardiac cycle, interoceptive accuracy and personality. Biol Psychol. 126, 19–29. [PubMed: 28385627]

Khalsa SS, Adolphs R, Cameron OG, Critchley HD, Davenport PW, Feinstein JS, Feusner JD, Garfinkel SN, Lane RD, Mehling WE, Meuret AE, Nemeroff CB, Oppenheimer S, Petzschner FH, Pollatos O, Rhudy JL, Schramm LP, Simmons WK, Stein MB, Stephan KE, Van den Bergh O, Van Diest I, von Leupoldt A, Paulus MP, Ainley V, Al Zoubi O, Aupperle R, Avery J, Baxter L, Benke

C, Berner L, Bodurka J, Breese E, Brown T, Burrows K, Cha Y-H, Clausen A, Cosgrove K, Deville D, Duncan L, Duquette P, Ekhtiari H, Fine T, Ford B, Garcia Cordero I, Gleghorn D, Guereca Y, Harrison NA, Hassanpour M, Hechler T, Heller A, Hellman N, Herbert B, Jarrahi B, Kerr K, Kirlic N, Klabunde M, Kraynak T, Kriegsman M, Kroll J, Kuplicki R, Lapidus R, Le T, Hagen KL, Mayeli A, Morris A, Naqvi N, Oldroyd K, Pané-Farré C, Phillips R, Poppa T, Potter W, Puhl M, Safron A, Sala M, Savitz J, Saxon H, Schoenhals W, Stanwell-Smith C, Teed A, Terasawa Y, Thompson K, Toups M, Umeda S, Upshaw V, Victor T, Wierenga C, Wohlrab C, Yeh H-W, Yoris A, Zeidan F, Zotev V, Zucker N, 2018. Interoception and Mental Health: A Roadmap. Biol Psychiatry Cogn Neurosci Neuroimaging. 3 (6), 501–513. [PubMed: 29884281]

Damasio A, Carvalho GB, 2013. The nature of feelings: evolutionary and neurobiological origins. Nat Rev Neurosci. 14 (2), 143–152. [PubMed: 23329161]

Wemmie JA, 2011. Neurobiology of panic and pH chemosensation in the brain. DialoguesClinNeurosci. 13, 475–483.

Muhtz C, Wiedemann K, Kellner M, 2012. Panicogens in patients with Post-Traumatic Stress Disorder (PTSD). Curr Pharm Des. 18, 5608–5618. [PubMed: 22632476]

Vollmer LL, Strawn JR, Sah R. Acid-base dysregulation and chemosensory mechanisms in panic disorder: A translational update. Transl Psychiatry. 2015;5.

Kellner M, Muhtz C, Nowack S, Leichsenring I, Wiedemann K, Yassouridis A, 2018. Effects of 35% carbon dioxide (CO 2) inhalation in patients with post-traumatic stress disorder (PTSD): A double-blind, randomized, placebo-controlled, cross-over trial. J Psychiatr Res. 96, 260–264. [PubMed: 29128558]

Leibold NK, van den Hove DLA, Viechtbauer W, Buchanan GF, Goossens L, Lange I, et al. CO2 exposure as translational cross-species experimental model for panic. Transl Psychiatry. 2016;6:e885. [PubMed: 27598969]

Ziemann AE, Allen JE, Dahdaleh NS, Drebot II, Coryell MW, Wunsch AM, Lynch CM, Faraci FM, Howard MA, Welsh MJ, Wemmie JA, 2009. The amygdala is a chemosensor that detects carbon dioxide and acidosis to elicit fear behavior. Cell. 139 (5), 1012–1021. [PubMed: 19945383]

McMurray KMJ, Gray A, Horn P, Sah R, 2020. High Behavioral Sensitivity to Carbon Dioxide Associates with Enhanced Fear Memory and Altered Forebrain Neuronal Activation. Neuroscience. 429, 92–105. [PubMed: 31930959]

Rassovsky Y, Kushner MG, 2003. Carbon dioxide in the study of panic disorder: Issues of definition, methodology, and outcome. J Anxiety Disord. 17 (1), 1–32. [PubMed: 12464286]

Vollmer LL, Ghosal S, McGuire JL, Ahlbrand RL, Li K-Y, Santin JM, Ratliff-Rang CA, Patrone LGA, Rush J, Lewkowich IP, Herman JP, Putnam RW, Sah R, 2016. Microglial Acid Sensing Regulates Carbon Dioxide-Evoked Fear. Biol Psychiatry. 80 (7), 541–551. [PubMed: 27422366]

Telch MJ, Rosenfield D, Lee H-J, Pai A, 2012. Emotional reactivity to a single inhalation of 35% carbon dioxide and its association with later symptoms of posttraumatic stress disorder and anxiety in soldiers deployed to Iraq. Arch Gen Psychiatry. 69 (11), 1161. 10.1001/archgenpsychiatry.2012.8. [PubMed: 23117637]

Coryell W, Pine D, Fyer A, Klein D, 2006. Anxiety responses to CO2 inhalation in subjects at high-risk for panic disorder. J Affect Disord. 92 (1), 63–70. [PubMed: 16527360]

Michopoulos V, Powers A, Gillespie CF, Ressler KJ, Jovanovic T, 2017. Inflammation in Fear-and Anxiety-Based Disorders: PTSD, GAD, and beyond. Neuropsychopharmacology. 42 (1), 254–270. [PubMed: 27510423]

Sumner JA, Nishimi KM, Koenen KC, Roberts AL, Kubzansky LD, 2020. Posttraumatic stress disorder and inflammation: untangling issues of bidirectionality. Biol Psychiatry. 87 (10), 885–897. 10.1016/j.biopsych.2019.11.005. [PubMed: 31932029]

Won E, Kim YK, 2020. Neuroinflammation-associated alterations of the brain as potential neural biomarkers in anxiety disorders. Int J Mol Sci. 21, 1–19.

Deslauriers J, Toth M, Der-Avakian A, Risbrough VB, 2018. Current Status of Animal Models of Posttraumatic Stress Disorder: Behavioral and Biological Phenotypes, and Future Challenges in Improving Translation. Biol Psychiatry. 83 (10), 895–907. [PubMed: 29338843]

Jones ME, Lebonville CL, Barrus D, Lysle DT, 2015. The Role Of Brain Interleukin-1 In Stress-Enhanced Fear Learning. Neuropsychopharmacology. 40 (5), 1289–1296. [PubMed: 25430780]

Furtado M, Katzman MA, 2015. Neuroinflammatory pathways in anxiety, posttraumatic stress, and obsessive compulsive disorders. Psychiatry Res. 229 (1–2), 37–48. [PubMed: 26296951]

van Duinen MA, Schruers KRJ, Kenis GRL, Wauters A, Delanghe J, Griez EJL, Maes MHJ, 2008. Effects of experimental panic on neuroimmunological functioning. 64 (3), 305–310.

Marques DA, Gargaglioni LH, Joseph V, Bretzner F, Bícego KC, Fournier S, Kinkead R, 2021. Impact of ovariectomy and CO2 inhalation on microglia morphology in select brainstem and hypothalamic areas regulating breathing in female rats. Brain Res. 1756, 147276. 10.1016/j.brainres.2021.147276. [PubMed: 33422531]

Johnson A, Gross P. Sensory circumventricular organs and brain homeostatic pathways. Faseb J. 1993;7:678–686. [PubMed: 8500693]

McKinley MJ, Denton DA, Ryan PJ, Yao ST, Stefanidis A, Oldfield BJ. From sensory circumventricular organs to cerebral cortex: Neural pathways controlling thirst and hunger. J Neuroendocrinol. 2019;31.

Matsuda T, Hiyama TY, Niimura F, Matsusaka T, Fukamizu A, Kobayashi K, Kobayashi K, Noda M, 2017. Distinct neural mechanisms for the control of thirst and salt appetite in the subfornical organ. Nat Neurosci. 20 (2), 230–241. [PubMed: 27991901]

Smith PM, Ferguson AV, 2010. Circulating signals as critical regulators of autonomic state–central roles for the subfornical organ. Am J Physiol Regul Integr Comp Physiol. 299 (2), R405–R415. [PubMed: 20463185]

Sisó S, Jeffrey M, González L, 2010. Sensory circumventricular organs in health and disease. Acta Neuropathol. 120 (6), 689–705. [PubMed: 20830478]

Goshen I, Kreisel T, Ounallah-Saad H, Renbaum P, Zalzstein Y, Ben-Hur T, et al. A dual role for interleukin-1 in hippocampal-dependent memory processes. Psychoneuroendocrinology;32:1106–1115.

Jones ME, Lebonville CL, Paniccia JE, Balentine ME, Reissner KJ, Lysle DT, 2018. Hippocampal interleukin-1 mediates stress-enhanced fear learning: A potential role for astrocyte-derived interleukin-1β. Brain Behav Immun. 67, 355–363. [PubMed: 28963000]

Rachal Pugh C, Fleshner M, Watkins LR, Maier SF, Rudy JW, 2001. The immune system and memory consolidation: A role for the cytokine IL-1β. Neurosci Biobehav Rev. 25 (1), 29–41. [PubMed: 11166076]

Swanson LW, Lind RW, 1986. Neural projections subserving the initiation of a specific motivated behavior in the rat: new projections from the subfornical organ. Brain Res. 379 (2), 399–403. [PubMed: 3742231]

Miselis RR, 1981. The efferent projections of the subfornical organ of the rat: a circumventricular organ within a neural network subserving water balance. Brain Res. 230 (1–2), 1–23. [PubMed: 7317773]

McKim DB, Weber MD, Niraula A, Sawicki CM, Liu X, Jarrett BL, Ramirez-Chan K, Wang Y, Roeth RM, Sucaldito AD, Sobol CG, Quan N, Sheridan JF, Godbout JP, 2018. Microglial recruitment of IL-1β-producing monocytes to brain endothelium causes stress-induced anxiety. Mol Psychiatry. 23 (6), 1421–1431. [PubMed: 28373688]

Liu X, Yamashita T, Chen Q, Belevych N, Mckim DB, Tarr AJ, Coppola V, Nath N, Nemeth DP, Syed ZW, Sheridan JF, Godbout JP, Zuo J, Quan N, 2015. Interleukin 1 Type 1 Receptor Restore: A Genetic Mouse Model for Studying Interleukin 1 Receptor-Mediated Effects in Specific Cell Types. J Neurosci. 35 (7), 2860–2870. [PubMed: 25698726]

DiSabato DJ, Nemeth DP, Liu X, Witcher KG, O'Neil SM, Oliver B, Bray CE, Sheridan JF, Godbout JP, Quan N, 2021. Interleukin-1 receptor on hippocampal neurons drives social withdrawal and cognitive deficits after chronic social stress. Mol Psychiatry. 26 (9), 4770–4782. 10.1038/s41380-020-0788-3. [PubMed: 32444870]

Taugher RJ, Lu Y, Wang Y, Kreple CJ, Ghobbeh A, Fan R, Sowers LP, Wemmie JA, 2014. The Bed Nucleus of the Stria Terminalis Is Critical for Anxiety-Related Behavior Evoked by CO2 and Acidosis. J Neurosci. 34 (31), 10247–10255. [PubMed: 25080586]

GRIEBEL GUY, BLANCHARD DCAROLINE., BLANCHARD ROBERTJ, 1996. Evidence that the behaviors in the mouse defense test battery relate to different emotional states: A factor analytic study. Physiol Behav. 60 (5), 1255–1260. [PubMed: 8916179]

Shansky RM, 2015. Sex differences in PTSD resilience and susceptibility: Challenges for animal models of fear learning. Neurobiol Stress. 1, 60–65. [PubMed: 25729759]

Biagioni AF, Anjos-Garcia TD, Ullah F, Fisher IR, Falconi-Sobrinho LL, Freitas R.L.d., Felippotti TT, Coimbra NC, 2016. Neuroethological validation of an experimental apparatus to evaluate oriented and non-oriented escape behaviours: Comparison between the polygonal arena with a burrow and the circular enclosure of an open-field test. Behav Brain Res. 298, 65–77. [PubMed: 26545831]

Schubert I, Ahlbrand R, Winter A, Vollmer L, Lewkowich I, Sah R, 2018. Enhanced fear and altered neuronal activation in forebrain limbic regions of CX3CR1-deficient mice. Brain Behav Immun. 68, 34–43. [PubMed: 28943292]

Liu X, Nemeth DP, McKim DB, Zhu L, DiSabato DJ, Berdysz O, Gorantla G, Oliver B, Witcher KG, Wang Y, Negray CE, Vegesna RS, Sheridan JF, Godbout JP, Robson MJ, Blakely RD, Popovich PG, Bilbo SD, Quan N, 2019. Cell-Type-Specific Interleukin 1 Receptor 1 Signaling in the Brain Regulates Distinct Neuroimmune Activities. Immunity. 50 (2), 317–333.e6. [PubMed: 30683620]

McMurray KMJ, Strawn JR, Sah R, 2019. Fluoxetine Modulates Spontaneous and Conditioned Behaviors to Carbon Dioxide (CO2) Inhalation and Alters Forebrain-Midbrain Neuronal Activation. Neuroscience. 396, 108–118. [PubMed: 30439538]

Paxinos G, Watson C, 1998. The mouse brain in stereotaxic coordinates. Academic Press, San Diego, CA.

Strawn JR, Vollmer LL, McMurray KMJ, Mills JA, Mossman SA, Varney ST, Schroeder HK, Sah R, 2018. Acid-sensing T cell death associated gene-8 receptor expression in panic disorder. Brain Behav Immun. 67, 36–41. [PubMed: 28736033]

Winter A, Ahlbrand R, Sah R, 2019. Recruitment of central angiotensin II type 1 receptor associated neurocircuits in carbon dioxide associated fear. Prog Neuro-Psychopharmacology Biol Psychiatry. 92, 378–386.

Bollinger JL, Horchar MJ, Wohleb ES, 2020. Diazepam limits microglia-mediated neuronal remodeling in the prefrontal cortex and associated behavioral consequences following chronic unpredictable stress. Neuropsychopharmacology. 45 (10), 1766–1776. [PubMed: 32454511]

Nakamori T, Sakata Y, Watanabe T, Morimoto A, Nakamura S, Murakami N, 1995. Suppression of interleukin-1β production in the circumventricular organs in endotoxin-tolerant rabbits. Brain Res. 675 (1–2), 103–109. [PubMed: 7796118]

Gorman JM, Papp LA, Coplan JD, Martinez JM, Lennon S, Goetz RR, et al. , 1994. Anxiogenic effects of CO2 and hyperventilation in patients with panic disorder. Am J Psychiatry. 151, 547–553. [PubMed: 8147452]

Papp LA, Klein DF, Gorman JM, 1993. Carbon dioxide hypersensitivity, hyperventilation, and panic disorder. Am J Psychiatry. 150, 1149–1157. [PubMed: 8392296]

Magnotta VA, Heo H-Y, Dlouhy BJ, Dahdaleh NS, Follmer RL, Thedens DR, Welsh MJ, Wemmie JA, 2012. Detecting activity-evoked pH changes in human brain. ProcNatlAcad Sci USA 109 (21), 8270–8273.

Loeschcke HH, 1982. Central chemosensitivity and the reaction theory. J Physiol. 332, 1–24. [PubMed: 6818338]

Dantzer R, 2009. Cytokine, Sickness Behaviour, and Depression. Immunol Allergy Clin North Am. 29, 247–264. [PubMed: 19389580]

Koo JW, Duman RS, 2009. Interleukin-1 receptor null mutant mice show decreased anxiety-like behavior and enhanced fear memory. Neurosci Lett. 456 (1), 39–43. [PubMed: 19429130]

Johnson AK, Gross PM, AK J, PM G. Sensory circumventricular organs and brain homeostatic pathways. FASEB J. 1993;7:678–686. [PubMed: 8500693]

McKinley MJ, McAllen RM, Davern P, Giles ME, Penschow J, Sunn N, et al. The sensory circumventricular organs of the mammalian brain. Adv Anat Embryol Cell Biol. 2003;172:III–XII, 1–122, back cover. [PubMed: 12901335]

McKinley MJ, Allen AM, Burns P, Colvill LM, Oldfield BJ, 1998. Interaction of circulating hormones with the brain: the roles of the subfornical organ and the organum vasculosum of the lamina terminalis. Clin Exp Pharmacol Physiol Suppl. 25 (S1), S61–S67. [PubMed: 9809195]

Ferguson AV, 2014. Circumventricular Organs: Integrators of Circulating Signals Controlling Hydration. Energy Balance, and Immune Function.

Mimee A, Smith PM, Ferguson AV. Circumventricular organs: Targets for integration of circulating fluid and energy balance signals? Physiol Behav. 2013. 28 February 2013. 10.1016/j.physbeh.2013.02.012.

Zimmerman Christopher A., Lin Yen-Chu, Leib David E., Guo Ling, Huey Erica L., Daly Gwendolyn E., Chen Yiming, Knight Zachary A., 2016. Thirst neurons anticipate the homeostatic consequences of eating and drinking. Nature. 537 (7622), 680–684. [PubMed: 27487211]

Hsu Ted M., Bazzino Paula, Hurh Samantha J., Konanur Vaibhav R., Roitman Jamie D., Roitman Mitchell F., 2020. Thirst recruits phasic dopamine signaling through subfornical organ neurons. Proc Natl Acad Sci U S A. 117 (48), 30744–30754. [PubMed: 33199591]

Ferguson Alastair V., Beckmann Leslie M., Fisher John T., 1989. Effects of subfornical organ stimulation on respiration in the anesthetized rat. Can J Physiol Pharmacol. 67 (9), 1097–1101. [PubMed: 2598133]

Wei Shun-Guang, Zhang Zhi-Hua, Beltz Terry G., Yu Yang, Johnson Alan Kim, Felder Robert B., 2013. Subfornical organ mediates sympathetic and hemodynamic responses to blood-borne proinflammatory cytokines. Hypertension. 62 (1), 118–125. [PubMed: 23670302]

Olff Miranda, Langeland Willie, Gersons Berthold P.R., 2005. The psychobiology of PTSD: Coping with trauma. Psychoneuroendocrinology. 30 (10), 974–982. [PubMed: 15964146]

Chiu GS, Chatterjee D, Darmody PT, Walsh JP, Meling DD, Johnson RW, Freund GG, 2012. Hypoxia/reoxygenation impairs memory formation via adenosine-dependent activation of caspase 1. J Neurosci. 32 (40), 13945–13955. [PubMed: 23035103]

Fanselow Michael S., 1994. Neural organization of the defensive behavior system responsible for fear. Psychon Bull Rev. 1 (4), 429–438. [PubMed: 24203551]

Paré Denis, Quirk Gregory J., Ledoux Joseph E., 2004. New vistas on amygdala networks in conditioned fear. J Neurophysiol. 92 (1), 1–9. [PubMed: 15212433]

Misslin René, 2003. The defense system of fear: Behavior and neurocircuitry. Neurophysiol Clin. 33 (2), 55–66. [PubMed: 12837573]

Maddox Stephanie A., Hartmann Jakob, Ross Rachel A., Ressler Kerry J., 2019. Deconstructing the Gestalt: Mechanisms of Fear, Threat, and Trauma Memory Encoding. Neuron. 102 (1), 60–74. [PubMed: 30946827]

Marek R, Strobel C, Bredy TW, Sah P, 2013. The amygdala and medial prefrontal cortex: partners in the fear circuit. J Physiol. 591, 2381–2391. [PubMed: 23420655]

Strobel C, Marek R, Gooch HM, Sullivan RKP, Sah P. Prefrontal and Auditory Input to Intercalated Neurons of the Amygdala. Cell Rep. 2015;10:1435–1442. [PubMed: 25753409]

Likhtik Ekaterina, Popa Daniela, Apergis-Schoute John, Fidacaro George A., Paré Denis, 2008. Amygdala intercalated neurons are required for expression of fear extinction. Nature. 454 (7204), 642–645. [PubMed: 18615014]

Sierra-Mercado Demetrio, Padilla-Coreano Nancy, Quirk Gregory J, 2011. Dissociable Roles of Prelimbic and Infralimbic Cortices, Ventral Hippocampus, and Basolateral Amygdala in the Expression and Extinction of Conditioned Fear. Neuropsychopharmacology. 36 (2), 529–538. [PubMed: 20962768]

Do-Monte FH, Manzano-Nieves G, Quinones-Laracuente K, Ramos-Medina L, Quirk GJ, 2015. Revisiting the Role of Infralimbic Cortex in Fear Extinction with Optogenetics. J Neurosci. 35 (8), 3607–3615. [PubMed: 25716859]

Gross Cornelius T., Canteras Newton Sabino, 2012. The many paths to fear. Nat Rev Neurosci. 13 (9), 651–658. [PubMed: 22850830]

Johnson Philip L., Hollis Jacob H., Moratalla Rosario, Lightman Stafford L., Lowry Christopher A., 2005. Acute hypercarbic gas exposure reveals functionally distinct subpopulations of serotonergic neurons in rats. J Psychopharmacol. 19 (4), 327–341. [PubMed: 15982987]

Floyd Nicole S., Price Joseph L., Ferry Amon T., Keay Kevin A., Bandler Richard, 2000. Orbitomedial prefrontal cortical projections to distinct longitudinal columns of the periaqueductal gray in the rat. J Comp Neurol. 422 (4), 556–578. [PubMed: 10861526]

Rizvi Tilat A., Ennis Matthew, Behbehani Michael M., Shipley Michael T., 1991. Connections between the central nucleus of the amygdala and the midbrain periaqueductal gray: Topography and reciprocity. J Comp Neurol. 303 (1), 121–131. [PubMed: 1706363]

Faull Olivia K., Subramanian Hari H., Ezra Martyn, Pattinson Kyle T.S., 2019. The midbrain periaqueductal gray as an integrative and interoceptive neural structure for breathing. Neurosci Biobehav Rev. 98, 135–144. [PubMed: 30611797]

Terpou Braeden A., Densmore Maria, Théberge Jean, Frewen Paul, McKinnon Margaret C., Nicholson Andrew A., Lanius Ruth A., 2020. The hijacked self: Disrupted functional connectivity between the periaqueductal gray and the default mode network in posttraumatic stress disorder using dynamic causal modeling. NeuroImage Clin. 27, 102345. 10.1016/j.nicl.2020.102345. [PubMed: 32738751]

Harricharan S, Rabellino D, Frewen PA, Densmore M, Théberge J, McKinnon MC, et al. , 2016. fMRI functional connectivity of the periaqueductal gray in PTSD and its dissociative subtype. Brain Behav. 6.

Webb Elisabeth K., Huggins Ashley A., Belleau Emily L., Taubitz Lauren E., Hanson Jessica L., deRoon-Cassini Terri A., Larson Christine L., 2020. Acute Posttrauma Resting-State Functional Connectivity of Periaqueductal Gray Prospectively Predicts Posttraumatic Stress Disorder Symptoms. Biol Psychiatry Cogn Neurosci Neuroimaging. 5 (9), 891–900. [PubMed: 32389746]

KYAW HLA, ZENG ZHIZHEN, SU KUI, FAN PING, SHELL BRENDA CARTER K, KENNETH C, LI YI, 1998. Cloning, characterization and mapping of human homolog of mouse T-cell death-associated gene. DNA Cell Biol. 17 (6), 493–500. [PubMed: 9655242]

Zhu Ling, Liu Xiaoyu, Nemeth Daniel P., DiSabato Damon J., Witcher Kristina G., Mckim Daniel B., Oliver Braedan, Le Xi, Gorantla Gowthami, Berdysz Olimpia, Li Jiaoni, Ramani Aishwarya D., Chen Zhibiao, Wu Dongcheng, Godbout Jonathan P., Quan Ning, 2019. Interleukin-1 causes CNS inflammatory cytokine expression via endothelia-microglia bi-cellular signaling. Brain Behav Immun. 81, 292–304. [PubMed: 31228609]

Costerousse O, Jaspard E, Wei L, Corvol P, Alhenc-Gelas F, 1992. The angiotensin I-converting enzyme (kininase II): molecular organization and regulation of its expression in humans. J Cardiovasc Pharmacol. 20 (Supplement 9), S10–S15. [PubMed: 1282623]

Kelly Megan M., Forsyth John P., Karekla Maria, 2006. Sex differences in response to a panicogenic challenge procedure: An experimental evaluation of panic vulnerability in a non-clinical sample. Behav Res Ther. 44 (10), 1421–1430. [PubMed: 16364237]

Quadt L, Critchley HD, Garfinkel SN, 2018. The neurobiology of interoception in health and disease. Ann N Y Acad Sci. 1428.

Feinstein Justin S, Buzza Colin, Hurlemann Rene, Follmer Robin L, Dahdaleh Nader S, Coryell William H, Welsh Michael J, Tranel Daniel, Wemmie John A, 2013. Fear and panic in humans with bilateral amygdala damage. Nat Neurosci. 16 (3), 270–272. [PubMed: 23377128]

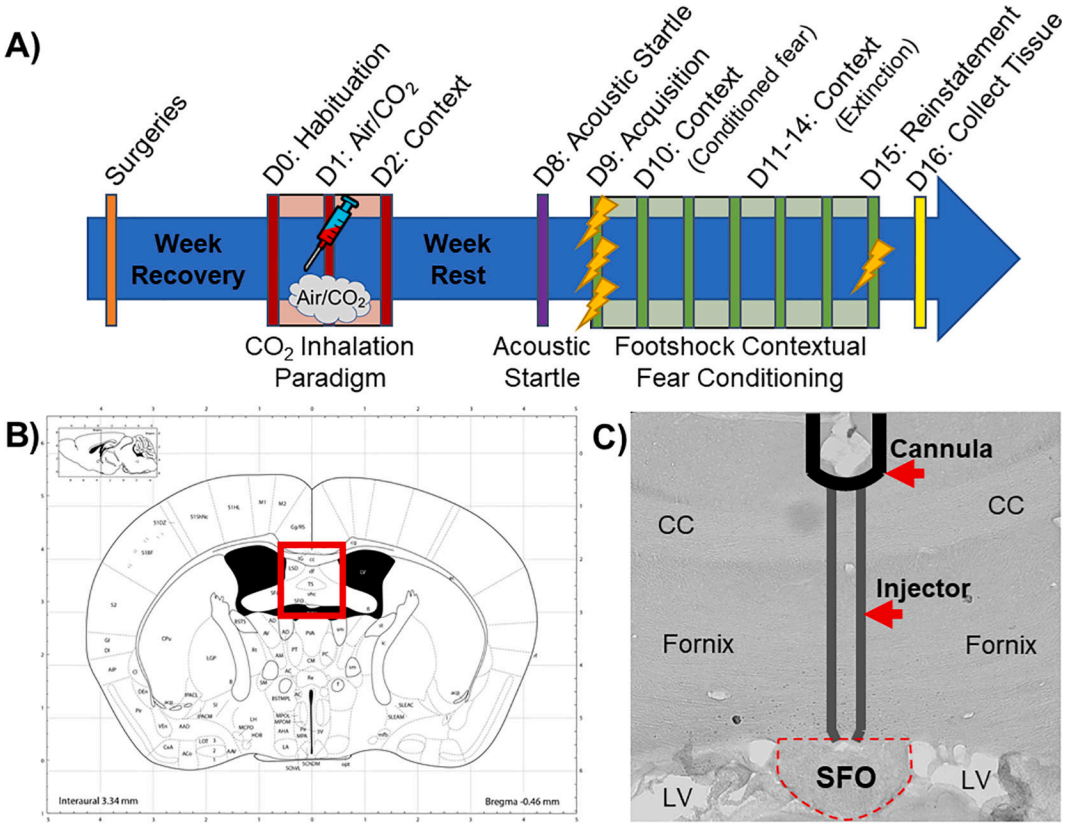

Fig. 1.

A) Schematic overview of the experimental timeline. Mice received cannulations targeting the subfornical organ (SFO) and were allowed to recover for 1 week before undergoing the CO_2 inhalation paradigm (see text for details). Mice received a single IL-1RA or vehicle infusion into the SFO 30 min prior to either CO_2 or air inhalation then were re-exposed to inhalation context the next day. Mice were left undisturbed for a week, after which they were exposed to the acoustic startle test followed by a contextual fear conditioning paradigm the next day (see text for details). Tissue was collected the day after all behavioral testing was completed. B) Image from brain atlas (Paxinos and Watson) showing location of the SFO (bregma. AP −0.48 mm, DV 2.4 mm, ML 0 mm). C) A representative image showing a SFO "hit" with injector tracts into the dorsal SFO. D = Day; CC = corpus callosum; LV = lateral ventricle.

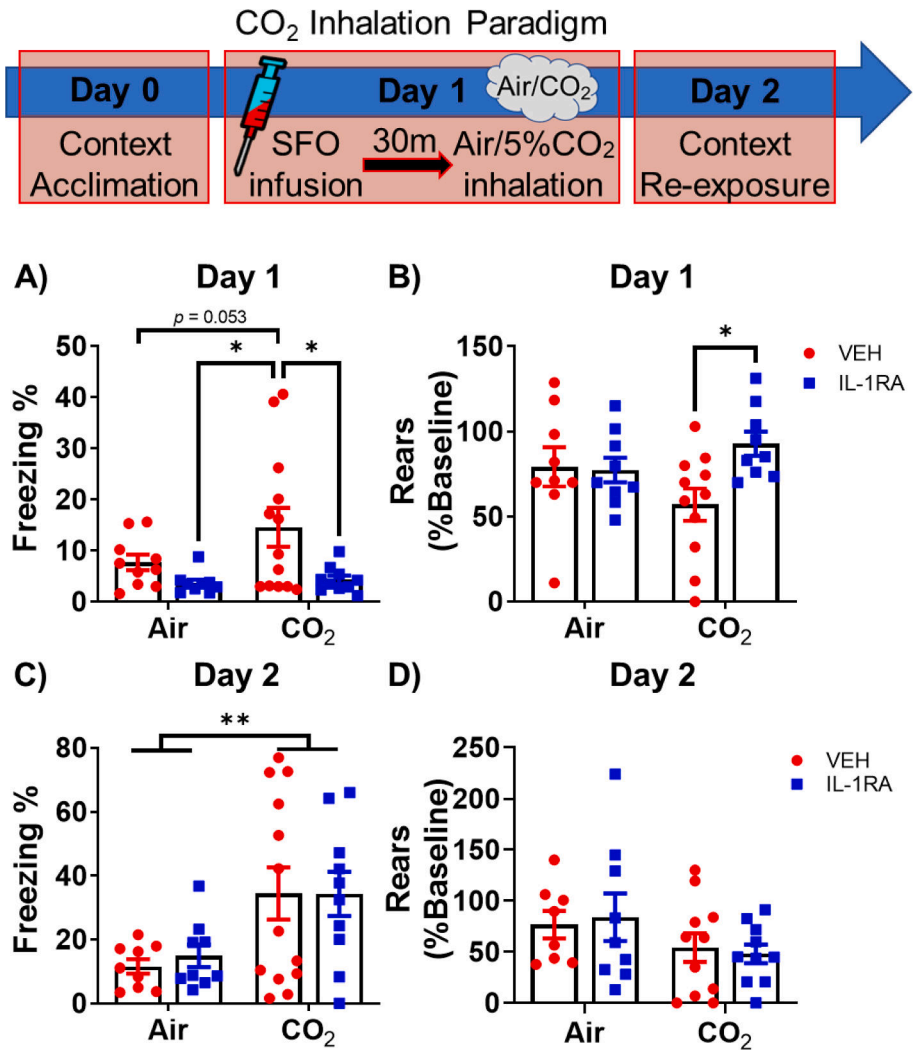

Fig. 2.

SFO- IL-1RA modulates active and passive defensive behaviors to CO_2 Inhalation. Top panel shows the CO_2 Inhalation paradigm. Mice received vehicle or IL-1RA into the SFO 30 min prior to CO_2 inhalation. Control mice received air inhalation. A) IL-1RA treatment reduced freezing to CO_2 inhalation. B) IL-1RA also restored reduction in rearing during CO_2 inhalation, while having no effect on rearing in air exposed mice. During Day 2 context re-exposure, no significant effects were observed on (C) freezing or (D) rearing behaviors between mice receiving IL-1RA or vehicle on Day 1. Data are mean ± SEM; *p < 0.05 **p < 0.01, p = 0.053 between Air and CO_2 vehicle groups (panel A) (n = 9–13/group).

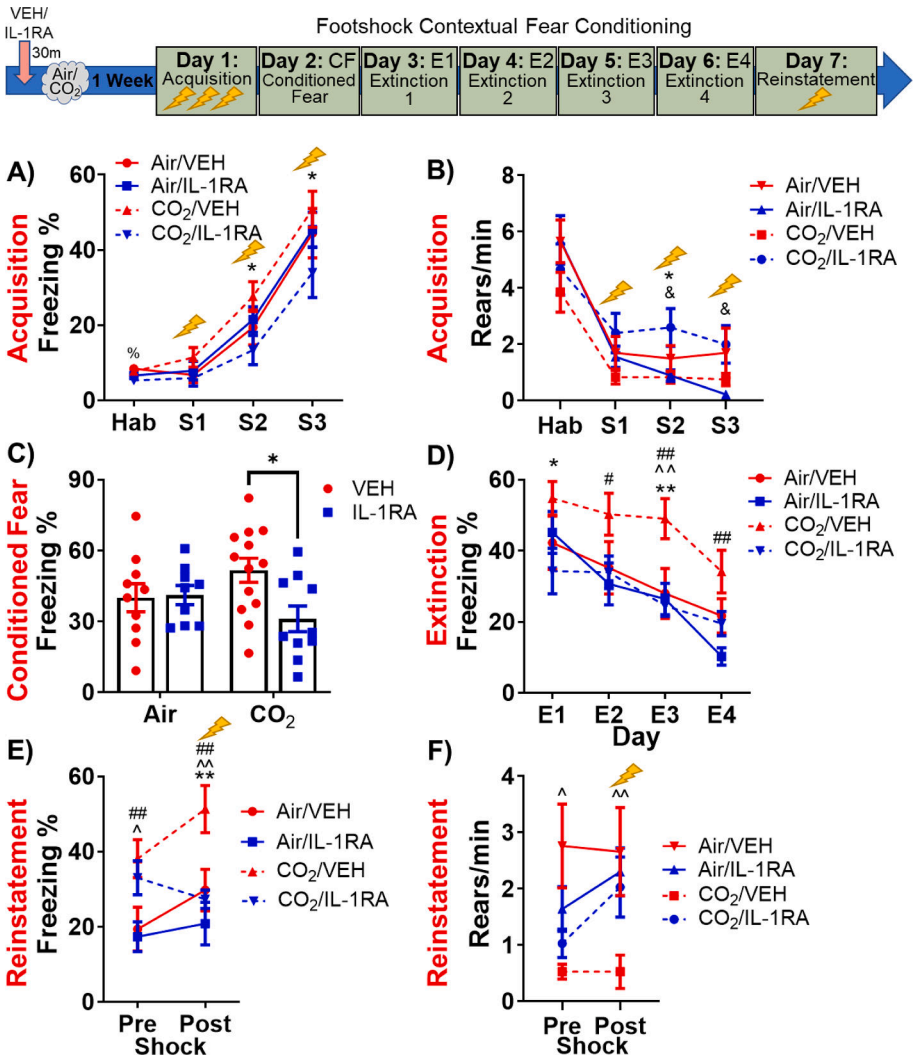

Fig. 3.

SFO-IL-1R1 signaling modulates delated effects of CO_2 on active and passive behaviors during contextual fear conditioning, extinction and reinstatement. Top panel shows the layout of the fear conditioning paradigm. See Fig. 1 for full experimental layout (mice received SFO-targeted infusions of IL-1RA or vehicle 30 min prior to CO_2 or air exposure *a week* prior to fear conditioning). A) On fear acquisition day, SFO-IL-1RA infusion one week earlier significantly reduced freezing following foot shocks only in mice previously exposed to CO_2 inhalation. No significant treatment effects were observed in air-exposed mice. B) In response to foot shock, prior IL-1RA treatment increased rearing in previously CO_2– exposed mice, but not air- exposed mice. C) Prior IL-1RA treatment attenuated conditioned freezing 24 h post-shock in previously CO_2– exposed mice, but not air-exposed mice. D) Prior IL-1RA treatment also attenuated the heightened freezing during extinction in CO_2-exposed mice, with no effects in air- exposed mice. Additionally, prior IL-1RA treatment attenuated freezing responses (E) and increased rearing responses (F) to a reminder foot shock during fear reinstatement only in mice previously exposed to CO_2 inhalation. Data are mean ± SEM. CO_2/VEH vs CO_2/IL-1RA: *p < 0.05 **p < 0.01;

CO_2/VEH vs Air/VEH: ^p < 0.05 ^^p < 0.01; CO_2/VEH vs Air/IL-1RA: $^{\#}$p < 0.05 $^{\#\#}$p < 0.01; Air/IL-1RA vs CO_2/IL-1RA: $^{\&}$p < 0.05; Air/VEH vs CO_2/IL-1RA: $^{\%}$p < 0.05. (n = 9–13) H = Habituation, S = Shock 1, 2, or 3, E = Extinction Day.

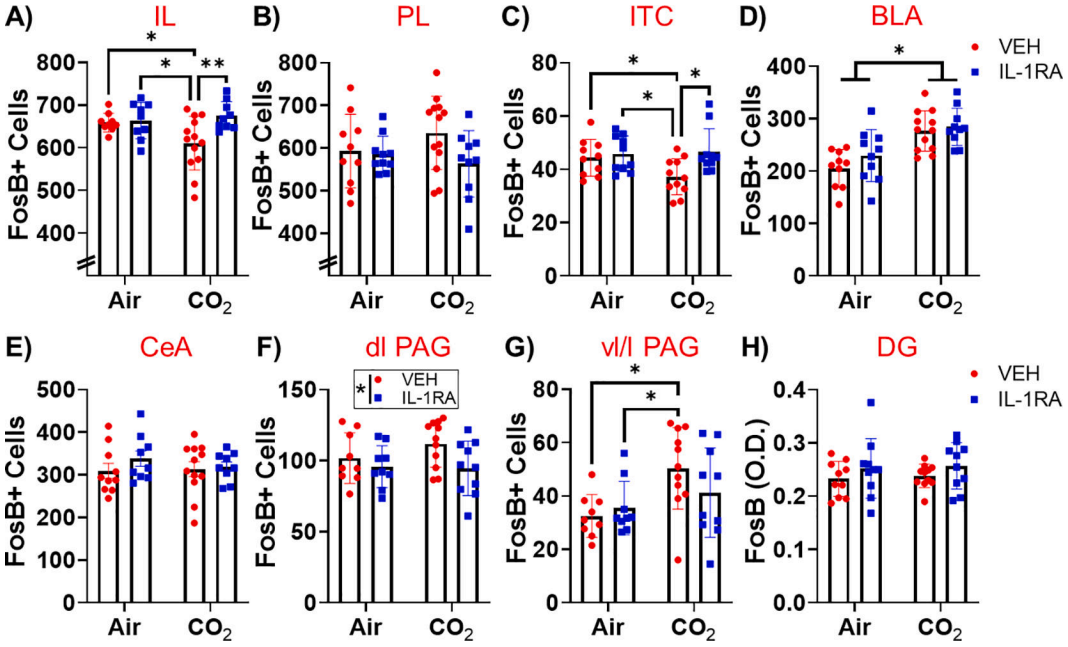

Fig. 4.

Post behavior regional ΔFosB + cell counts in CO_2– or air- exposed mice treated with vehicle or IL-1RA. (A) Within infralimbic cortex (IL), IL-1RA restored the CO_2 attenuation of FosB + cell counts. (B) Neither CO_2 or IL-1RA affected FosB + cell counts in the prelimbic cortex (PL). (C) Within the intercalated cells of the amygdala (ITC), IL-1RA restored the CO_2 attenuation of FosB + cell counts. (D) CO_2 inhalation increased basolateral amygdala (BLA) FosB + cell counts, but there was no effect of IL-1RA. (E) Neither CO_2 or IL-1RA affected FosB + cell counts in the central amygdala (CeA). (F) IL-1RA reduced FosB + cell counts in the dorsolateral periaqueductal grey (dl PAG). (G) CO_2 inhalation increased FosB + cell counts in the ventrolateral/lateral PAG (vl/l PAG) and CO2/VEH mice showed increased FosB + cell counts compared to Air/VEH and Air/IL-1RA mice. (H) Neither CO_2 or IL-1RA affected FosB + cell counts in the dentate gyrus of the hippocampus (DG). Data are mean ± SEM. *p < 0.05 **p < 0.01 (n = 8–13).

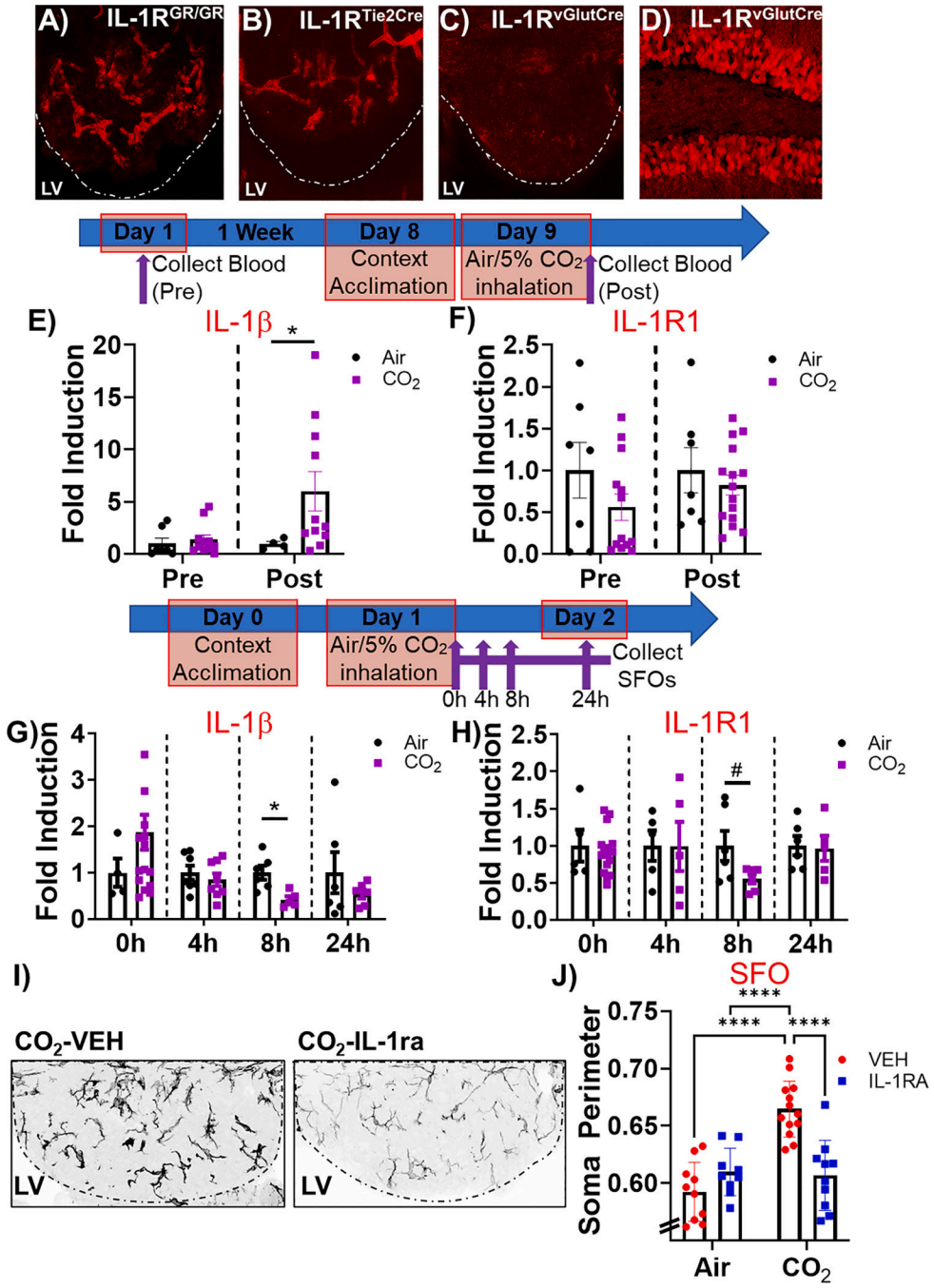

Fig. 5.

Endothelial localization of SFO IL-1R1 and CO2 mediated regulation of IL-1β/IL-1R1 expression. A) tdTomato fluorescence was observed in blood vessels within the SFO in IL-1R1$^{GR/GR}$ mice (global expression of IL-1R1). B) A similar tdTomato distribution was observed in SFO slices from Tie2Cre-IL-1R1$^{r/r}$ mice (endothelial-specific expression of IL-1R1). In Vglut2Cre-IL-1R1$^{r/r}$ mice that have neuron-specific expression of IL-1R1, no signal was observed in (C) the SFO, while there was high neuronal expression within (D) hippocampal dentate neurons. Timeline for blood collection for monocytic IL-1β/IL-1R1

expression: Blood was collected before and after air or CO_2 inhalation and IL-1β/IL-1R1 expression was quantified in enriched monocytes by RTqPCR. E) While there were no differences between air and CO_2 at baseline, CO_2 inhalation significantly increased IL-1β expression compared to air- exposed mice. F) No significant differences were observed in IL-1R1 expression between CO_2 and air groups at either time. Within the SFO, (G) IL-1 β expression was significantly reduced 8 h post CO_2 inhalation with no significant effects at other time points. H) SFO IL-1R1 expression was markedly reduced at 8 h following CO_2 inhalation, however significance was not attained. I) IL-1RA infusion significantly attenuated morphological activation of microglia in CO_2-exposed mice. Representative SFO IBA-1 stained images from CO_2-exposed vehicle and IL-1RA treated mice. J) Quantification of soma size revealed significant reduction in IL-1RA treated mice compared to vehicle (VEH) treated mice in mice previously exposed to CO_2 inhalation, but not air. *$p < 0.05$ ****$p < 0.0001$ $^{\#}p = 0.08$. Data are mean ± SEM. RTqPCR (Blood: IL-1 β (n = 4–11), IL-1R1 (n = 7–15); SFO: IL-1 β (n = 4–16), IL-1R1 (n = 5–16)); SFO IBA-1 (n = 9–13).

Table 1

Correlation analysis of freezing during testing phases of the Air/CO_2 inhalation paradigm (upper panel) and Footshock contextual Fear conditioning (lower panel) with delta FosB cell counts in the infralimbic (IL) cortex, Intercalated cell cluster of the amygdala (ITCs), dorsal lateral periaqueductal gray (dl PAG) and ventrolateral/lateral periaqueductal gray (vl/l PAG).

		FosB + Cells (IL Cortex)				*FosB + Cells (ITCs of Amygdala)*				*FosB + Cells (dl PAG)*				*FosB + Cells (vl/l PAG)*			
Paradigm	**Phase (%Freezing)**	**N**	**Pearson r**	**p value**	**95% CI**	**N**	**Pearson r**	**p value**	**95% CI**	**N**	**Pearson r**	**p value**	**95% CI**	**N**	**Pearson r**	**p value**	**95% CI**
Air/CO_2 Inhalation	Air/CO_2 Inhalation	39	−0.277	0.088$^{\#}$	−0.545 to 0.043	39	−0.137	0.405	−0.434 to 0.187	37	0.302	0.069$^{\#}$	−0.024 to 0.571	38	0.089	0.595	−0.237 to 0.397
	Context Re-exposure	39	−0.268	0.099$^{\#}$	−0.538 to 0.051	39	−0.005	0.976	−0.320 to 0.311	37	−0.061	0.720	−0.378 to 0.268	38	−0.058	0.732	−0.370 to 0.267
Footshock Contextual Fear Conditioning	Acquisition (avg shocks)	39	−0.173	0.292	−0.463 to 0.151	39	−0.289	0.075$^{\#}$	−0.554 to 0.030	37	−0.026	0.880	−0.347 to 0.301	38	−0.075	0.654	−0.386 to 0.251
	Conditioned Fear	39	−0.174	0.289	−0.464 to 0.149	39	−0.216	0.186	−0.498 to 0.106	37	0.284	0.089$^{\#}$	−0.044 to 0.557	38	0.049	0.771	−0.275 to 0.363
	Early Extinction (E1-E2)	39	−0.161	0.327	−0.454 to 0.163	39	−0.267	0.101	−0.537 to 0.053	37	0.296	0.075$^{\#}$	−0.031 to 0.566	38	0.174	0.297	−0.155 to 0.468
	Late Extinction (E3-E5)	39	−0.382	**0.016***	−0.623 to −0.076	39	−0.438	**0.005****	−0.662 to −0.142	37	0.289	0.083$^{\#}$	−0.039 to 0.560	38	0.346	**0.034***	0.029 to 0.599
	Reinstatement	39	−0.534	**0.001*****	−0.727 to −0.262	39	−0.464	**0.003****	−0.680 to −0.173	37	0.310	0.061$^{\#}$	−0.015 to 0.576	38	0.300	0.067$^{\#}$	−0.021 to 0.566

* $p < 0.05$

** $p < 0.01$

*** $p < 0.001$

$^{\#}$ $p < 0.10$.

Brain Behav Immun. Author manuscript; available in PMC 2023 March 01.